Article

Near-Infrared Spectroscopy of 2-Month Exercise Intervention Effects in Sedentary Older Adults With Diabetes and Mild Cognitive Impairment

Fei Zhao[1], Machiko Tomita[1] and Anirban Dutta[2*]

[1] Department of Rehabilitation Science, School of Public Health and Health Professions, University at Buffalo, Buffalo, New York 14214, USA.
[2] School of Engineering, University of Lincoln, Lincoln, LN67TS, UK.
* Correspondence: Correspondence: Anirban Dutta, adutta@case.edu

Abstract

The Global Burden of Disease Study (GBD 2019 Diseases and Injuries Collaborators) found that diabetes significantly increases the overall burden of disease, leading to a 24.4% increase in disability-adjusted life years. Persistently high glucose levels in diabetes can cause structural and functional changes in proteins throughout the body, and the accumulation of protein aggregates in the brain is associated with the progression of Alzheimer's Disease (AD).

To address this burden of type 2 diabetes mellitus (T2DM), a combined aerobic and resistance exercise program was developed based on the recommendations of the American College of Sports Medicine. The prospectively registered clinical trials (https://www.clinicaltrials.gov/ct2/show/NCT04626453, https://www.clinicaltrials.gov/ct2/show/NCT04812288) involved two groups: an Intervention group of older sedentary adults with T2DM and a Control group of healthy older adults who could be either active or sedentary. The completion rate for the 2-month exercise program was high, with participants completing on an average of 89.14% of the exercise sessions. This indicated that the program was practical, feasible, and well-tolerated, even during the COVID pandemic. It was also safe, requiring minimal equipment and no supervision. The exercise instructions were easy to understand, making them suitable for older adults with cognitive decline.

The near-infrared spectroscopy (NIRS) based brain and muscle oxygenation study provided evidence on brain overactivation among older adults with T2DM, supporting the compensatory theory. It also demonstrated that the 2-month combined exercise intervention effectively reduced brain overactivation and contributed to improved cognitive function. Operational modal analysis showed an exercise-related effect on the very low-frequency hemodynamic oscillations cluster, which may be associated with better vascular muscle and/or perivascular neurogenic regulation. Furthermore, we personalized the exercise duration and interval based on muscle oxygenation during physical tasks, leading to improvements in muscle oxidative capacity within just two months. This finding has practical implications for physical therapists, as they can target muscle oxygenation changes during physical tests to prescribe appropriate exercise doses for enhancing physical performance.

 doi:10.20944/preprints202306.0764.v1

Keywords: type 2 diabetes mellitus; functional near-infrared spectroscopy; muscle near-infrared spectroscopy; cognitive impairment; operational modal analysis

1 Introduction

The Global Burden of Disease Study (GBD 2019 Diseases and Injuries Collaborators) showed that diabetes significantly increases the burden of disease, with a 24.4% increase in age-standardized disability-adjusted life years [1]. Additionally, projections from the Centers for Disease Control and Prevention indicate that the burden of Alzheimer's Disease Related Dementias (ADRDs) in the United States is expected to double by 2060. Here, persistently elevated glucose levels in diabetes can lead to structural and functional changes in proteins throughout the body, and the spread of protein aggregates in the brain is implicated in the progression of Alzheimer's Disease (AD) [2]. According to the American Diabetes Association [3], adults with all types of diabetes should participate in more than 150 minutes of moderate intensity physical activity weekly for at least three days a week. However, previous research has shown that only 25% of older adults with diabetes met this recommendation [4], which can be due to low physical performance threshold, poor cardiorespiratory fitness, and other functional limitations in older adults with type 2 diabetes mellitus (T2DM) [5],[6],[7]. Older adults with T2DM often lack stamina and feel tired during prolonged single-time exercise, which may lead to a cessation of exercise training and obesity [8],[9]. Therefore, older adults with T2DM often become sedentary resulting in decline in their physical conditions [10]. In principal accordance, adjusting the intensity of the regular exercise programme to fit T2DM individual’s capacity should be investigated to change this vicious cycle. In the current study, considering the reduced capacity in sedentary older adults with T2DM, low to moderate intensity exercise may be appropriate; however, beneficial effects on the brain and muscle need to be established. Previous studies demonstrated that frequent but short single training sessions at moderate intensity can promote insulin sensitivity and reduce fatigue in older adults with T2DM [11] while improving muscle mitochondrial capacity [12] though the evidence is still limited. In young adults, researchers have developed individualised duration for a single exercise session and then multiple sets of exercise session based on the changes in the muscle oxygen level (oxygenation) during physical tasks and recovery stages [13],[14]. Here, the superiority of multiple exercise sets compared with a single set may help to determine appropriate exercise programme even for older adults. Since older adults with T2DM lack endurance and quickly fatigue [15] so exercising at shorter duration and longer intervals may fit into their cardiac capacity which may lead to good adherence. Therefore, in the current study, we aimed to study muscle and brain oxygenation changes to 2-month exercise intervention in sedentary older adults with diabetes and cognitive impairment that may help determine exercise effectiveness at a low to moderate intensity.

Studies on cognition in T2DM found that diabetes is pathophysiologically associated with cognitive decline [16],[17],[18]. Here, deficits in the structure and function of the

 doi:10.20944/preprints202306.0764.v1

prefrontal cortex are linked to reduced executive functions and poor glycaemic control in T2DM [19]. In neurocognitive aging, the compensatory hypothesis states that age-related overactivation is compensatory which is expressed by larger changes in oxyhemoglobin (oxyHb) with aging when processing cognitive tasks [20]. Several studies demonstrated that brain overactivation, especially in the dorsolateral prefrontal cortex (DLPFC) while performing working memory tasks occurs in T2DM [21],[22],[23]. Here, the pattern of brain overactivation may be related to the dysfunction of the neurovascular coupling (NVC)-cascade [24]. In the NVC-cascade, the cerebrovascular reactivity to cognitive load may be dysfunctional where cerebral blood flow (CBF) increases due to brain activity [25],[26],[27]. This increase in blood flow at the neuronally activated brain areas is the physiological basis for most functional neuroimaging techniques. With the increase in CBF, the cerebral metabolic rate of oxygen (CMRO2) increases [28] that is also influenced by the oxygen extraction fraction (OEF) [29]. The increase in CBF is roughly twice that of the increase in CMRO2 to keep the partial pressure of the oxygen in the tissue at a steady level [30],[31],[32]. Here, OEF can be altered in older adults with T2DM that can reduce task tolerance [33] where moderate-intensity training can be helpful [34],[35]. T2DM patients have been found to have dysregulated systemic hemodynamics during metaboreflex with an exaggerated blood pressure response and vasoconstriction in muscle [36] and brain [37]. Also, studies demonstrated reduced CBF with increasing age as one cause of cognitive impairment [38] as well as altered cerebral metabolism that can be addressed with physical activity and exercise [39]. Here, limited evidence shows that exercise can reverse brain overactivation in older adults, e.g., a study reported decreased brain activation in related cortical regions during a semantic memory-related task among older adults with mild cognitive impairment after a 12-week walking intervention [40]. Another study demonstrated that prefrontal brain activation was reduced after a combined exercise program in frail older adults [41]. However, currently there are no research studies examining the effect of exercise on reversing brain activation deficits and further improving cognition in older adults with T2DM. In this study, we postulated that 2-month exercise intervention in sedentary older adults with diabetes and cognitive impairment can attenuate prefrontal overactivation during Mini-Cog tasks [42]. Here, Mini-Cog test was suitable for rapid evaluation of cognition with a sensitivity of 76% and specificity of 73% [42] which may be improved by combining with portable brain imaging measures [43].

In this study, the cerebral oxyhemoglobin (oxyHb) and deoxyhemoglobin (deoxyHb) changes to Mini-Cog tasks and muscle oxygen saturation (SmO2) changes to biped tasks were measured with the near infrared spectroscopy (NIRS) technique [43]. Many studies [44],[45],[46] have demonstrated the adaptation of skeletal muscles to acute exercise and exercise training that can ameliorate metabolic dysfunction and prevent chronic disease [47]. Here, the metabolism in slow-twitch oxidative skeletal muscle may be the key for understanding the response to low-intensity physical activity in T2DM [10] in terms of dose response measured with muscle NIRS [48]. The muscle NIRS method has been used to diagnose various diseases and has developed rapidly in the last 20 years for measuring changes in myoglobin oxygenation level in skeletal muscle [48]. The muscle NIRS

 doi:10.20944/preprints202306.0764.v1

measurements estimate how oxygen delivery meets oxygen utilisation during exercise [48]. Here, muscle NIRS technique delivers near-infrared (NIR) light at wavelengths ranging from 650 to 900 nm into the muscle tissue and measures the amount of scattered light to estimate the muscle tissue properties. Different levels of SmO2 cause varied absorption rates in muscle tissues where the concentrations of two states of haemoglobin plus myoglobin, bound to oxygen and unbound to oxygen, in the tissue can be measured [49],[50],[51]. Muscle oxygen saturation, known as SmO2, is calculated as the percentage of oxygen bound in the total haemoglobin plus myoglobin concentration. In recent years, muscle NIRS has been used in clinical studies among people with chronic diseases, including patients with muscle myopathies [52], peripheral arterial disease [53],[54], muscle atrophy in multiple sclerosis patients [55], heart failure [56],[57], by measuring the match between oxygen delivery and utilisation. Some studies utilising muscle NIRS techniques analyse tissue oxygenation changes after an incremental power test to find the exercise threshold [58],[45],[59],[60]. For example, a study used the difference between oxy hemoglobin plus myoglobin and deoxy hemoglobin plus myoglobin to detect the time point at which the athletes reached the plateau at the physiological level [59]. Moreover, our previous study [61] exhibited a significant and positive correlation between the oxidative capacity expressed by changes in SmO2 and physical performance, including balance, gait speed, and endurance during a one-time low intensity heel raise physical stimulus among older adults. We developed a normalised SmO2 change rate (NSmO2 rate) [61], that is, a ratio between the rate of SmO2 drop to the amount of exercise, expressed by a SmO2 drop slope (numerator) and the duration of exercise (denominator). The slope of SmO2, defined by the difference between maximum SmO2 and minimum SmO2 divided by the time to reach minimum SmO2, was calculated by linear regression that corresponded with local perfusion [60]. Older adults with higher local perfusion [60] can have a better match between oxygen delivery and oxygen utilisation, and they showed an increased level of physical performance. However, the relationship between disease pathology and vascular problems with respect to SmO_2 and cerebral oxyHb among patients with diabetes is unclear [62],[63]. Here, endothelial vascular function and the capacity to increase cardiac output during exercise can be impaired in T2DM [63]. Also, impaired vasodilation [64],[65], especially homogenous blood flow distribution within the microvasculature, can be promoted by the mechanical properties of the endothelial glycocalyx [66]. Here, endothelial glycocalyx can be a shield against diabetic vascular complications [67] that can be affected by acute exercise induced responses especially at high-intensity interval exercise-induced oxidative stress [68]. Then, the maximal exercise capacity was found to be positively associated with the microvascular glycocalyx thickness at baseline [69] and a deteriorated glycocalyx could initiate cardiovascular disease pathology [70]. Therefore, individualized dosing of physical and cognitive exercises may be key when shedding of glycocalyx components is an ubiquitous process that can change the physiology of the endothelium during dose response [71]. Then, animal study has shown a reduction of the glycocalyx length with diabetes progression that correlated with an increasing level of glycated haemoglobin and decreased endothelial nitric oxide (NO) production [72] that can affect vascular tone [73] and vasomotion [74] – an emergent phenomena [75] – where optimal

 doi:10.20944/preprints202306.0764.v1

exercise can facilitate laminar shear for enhanced endothelial function [76]. Also, NO signaling participate in the mitochondrial respiration and biogenesis where a decline in physical performance and an increase in fatigue among individuals with T2DM can be partially due to reduced oxidative phosphorylation [77]. Oxidative phosphorylation produces energy or adenosine triphosphate (ATP) in the mitochondria in the presence of oxygen [78] and the ability of oxidative phosphorylation reflects oxidative capacity [79] where previous research has shown that individuals with T2DM had reduced oxidative capacity and low tolerance to exercise [80]. The exercise intervention was identified as an effective way to reverse this situation and improve oxidative capacity, further enhance physical performance, and relieve fatigue [40],[41].

Endothelial NO production [72] due to mechanotransduction at the endothelial glycocalyx [66] can affect vascular rhythmic activity [74], even in the absence of neural activity, especially in small vessels (<0.3mm) [81] enhanced by the nonlinear rheology of blood [82]. In our prior work [81], we found that blood vessel oscillations, measured with functional near-infrared spectroscopy (fNIRS), had a lower relative power in 0.01-0.052 Hz frequency band in the elderly subjects with T2DM when compared to age-matched controls during Mini-Cog three-item recall test. Here, potential reasons for <0.1Hz oscillations can be impaired small vessel function due to dysfunctional cytosolic oscillator, membrane oscillator, metabolic oscillator [83], vasoactive signaling [84], and smooth muscle autonomic innervation (0.021-0.052 Hz). Then, the biomechanical properties of the endothelial glycocalyx [85] may determine the Fahræus-Lindqvist-driven oscillations in the small vessels (<0.3mm) [81] that are solely due to the non-linear rheological properties of blood [86] flowing through the microvascular networks [87]. Therefore, fNIRS can measure the global oscillatory behavior of the microvascular network where dysfunction can be investigated [81] using operational modal analysis [88] of the flow-induced vibration. Here, pulsatility of the large blood vessels shows stiffening that's unable to cushion the pulsatile blood flow [89] while the Fahræus-Lindqvist-driven oscillations in the small blood vessels may be crucial for microvascular health including endothelial glycocalyx protection [90],[91] in hyperglycemia [92]. Moreover, endothelial glycocalyx promotes homogenous blood flow distribution within the microvasculature [66] that is crucial for the homogeneous diffusion of metabolites in the neurovascular tissue [81]. In the current study, changes in the prefrontal oxyhemoglobin (oxyHb) and deoxyhemoglobin (deoxyHb) concentration during Mini-Cog from resting levels were used for brain monitoring that was motivated by the prior work on fNIRS during memory encoding and retrieval in healthy [93]. Jahani et al [93] showed activation of the left dorsolateral prefrontal cortex during memory encoding while memory recalling resulted in activation in dorsolateral prefrontal cortex bilaterally. In the current study, we aimed to examine the effect of 2-month moderate-intensity aerobic and resistance exercise on muscular oxygen saturation (SmO2) changes to physical activity, prefrontal oxyHb and deoxyHb changes to cognitive activity, and operational modal analysis of hemodynamic response to cognitive activity using Covariance-Driven Stochastic Subspace Identification (SSI-COV) method [94] where the unknown neurovascular inputs to evoke the hemodynamic response were considered as realizations of white noise processes.

 doi:10.20944/preprints202306.0764.v1

2 Methods

2.1 Study Design

Our experimental study has two groups (see Figure 3): one Intervention group of older sedentary adults with T2DM (N=20) and one Control group (N=40) of healthy older adults who can be active or sedentary. Control groups, active (N=20) and sedentary healthy (N=20), were age and sex-matched with the Intervention group. For age matching, everyone in the control group was within a two-year difference from the matched person in T2DM group. Only older adults with T2DM received our 2-month exercise intervention and were evaluated at baseline and follow-up. The Control group did not perform our exercise intervention and was evaluated only once. Both baseline and follow-up data from the T2DM were compared with each other as well as with the one-time data from the Control group. The intervention T2DM group performed a moderate intensity resistance exercise and walked faster than usual on every alternate day for six days a week, as described next. They were contacted every two weeks by phone for encouragement to continue the exercise programme. Our current study is based on the prospectively registered clinical trials (https://www.clinicaltrials.gov/ct2/show/NCT04626453, https://www.clinicaltrials.gov/ct2/show/NCT04812288) that are published in the doctoral thesis of the first author, Fei Zhao [95].

2.2 2-month Exercise Intervention

Based on the American College of Sports Medicines (ACSM) [96], participants performed combined aerobic and resistance exercise, which consisted of progressive resistance exercise and walking at a faster speed than leisure walking i.e. at a moderate intensity, for six days/week. Participants were encouraged to do progressive resistance exercises and walk for about 20 minutes a day. Progressive resistance exercise was suggested to be performed every other day for three days a week and walking as aerobic exercise was on alternate days for three days a week for about 20 minutes a day. The subjects decided which day they perform and not perform the exercises. Here, ACSM [96] suggested an exercise set of 8–12 repetitions for 8–10 exercises, which involves major muscle groups and 10-15 repetitions for progression. Intensity and progression were tailored for older adults with T2DM. We reduced the number of movements to four in our study, including knee extension and flexion with ankle weights for both the legs, chair-stand and heel raises with the support of a chair or table. Based on a systematic review of progressive exercise, these movements were suggested for T2DM patients to lower blood glucose levels [97]. One-minute stretching was recommended as a warm-up before the four movements. Each movement was suggested to be performed in 3-4 sets, and the participants had an average 30-second break between the sets.

To determine the baseline optimal intensity of exercise, we let participants choose a comfortable ankle weight for knee flexion and extension and tested the maximum number for both the movements. For weeks 1 to 4, the repetitions for each set were 50% of the

 doi:10.20944/preprints202306.0764.v1

maximum. Weeks 1 and 2 had three sets that increased to four sets for weeks 3 and 4. From week 5, the number of repetitions in each set exceeded 60% of the maximum number. Weeks 7 and 8 were three sets and increased to four sets for weeks 7 and 8. The maximum number was tested for the chair-stand, and the same progression was applied without using ankle weights. The participants had a 30-second rest between the sets of three movements. In terms of heel raise, we obtained the maximum number of heel raises from the bilateral heel raise test during the baseline evaluation. A marker was placed on the wall above the participants' heads at the maximum height, and they were encouraged to reach the maximum height each time. Furthermore, the resting time was identified for participants' muscles to recover back to the baseline SmO2 level. Resting time between each set was given at an individual level for heel raises. Each session took approximately 15-20 minutes.

For walking intervention, walking at a brisk pace is a moderate-intensity exercise. First, the heart rate reserve (HRR) was calculated using the maximum and resting heart rates. The maximum walking speed was acquired from the 6-minute walking test (6MWT) where we measured their heart rate right after the 6MWT. At weeks 1 and 2, participants started at their 60% HRR and then increased to 65%, 70% to 75% of their HRR every two weeks. The total duration for one session of resistance exercise or walking was 8-15 minutes. We suggested that participants walk indoors in their dining room or other places with ample space and sufficient light. It was recommended to avoid carpets which can cause them to fall. If the distance in the dining room was too short, we suggested walking between rooms. The duration of the daily exercise containing two sessions was 152-256 minutes. In addition to resistance exercise, the weekly exercise was 120-180 minutes. However, depending on the individuals, this guideline was adjusted to their strengths or weaknesses, willingness, and progression. One-time walking or resistance training was considered one session and the total number of sessions was 96. The details are published in the doctoral thesis of the first author, Fei Zhao [95].

2.3 Sample

The sample size was determined by power analysis using the expected medium-large effect size from preliminary study (f=0.36) [61] at a significance level to achieve 80% statistical power. The recruitment considered a 20% attrition and screening failure rate in the diabetes group and a 10% screening failure in the control groups – please see the CONSORT flow diagram in Figure 3. For the Intervention group of older sedentary adults with T2DM, we recruited 32 participants, but 11 participants (34%) dropped out before follow-up because of COVID, or health conditions not related to COVID, and one did not complete the follow-up assessment. For the Control group, 118 were found eligible, 49 were matched with T2DM group and the data from 40 people were matched for the follow-up. A higher dropout rate occurred in our study than expected was partly due to the COVID. The demographic information is provided in Table 1.

Preprints (www.preprints.org) | NOT PEER-REVIEWED | Posted: 12 June 2023 doi:10.20944/preprints202306.0764.v1

Table 1. Demographic information

Characteristics	**Intervention group at baseline** **M(SD)**	**Sedentary healthy Control group** **M(SD)**	**Active healthy Control group** **M(SD)**	**F or χ^2**
Age	66.1 (4.5)	66.6 (4.2)	65.9 (4.2)	F = .055 (p=.947)
BMI	34.8 (4.8)	33.3 (5.3)	26.1 (4.3)***	F = 18.775*** (p<.001) Intervention group at baseline versus Active healthy Control group
Sex Male Female	 50.0% 50.0%	 50.0% 50.0%	 50.0% 50.0%	 χ^2 = 1.0 (p=1.000)

* p <.05, ** p<.01, *** p<.001
For chi-squares, * indicates the standard residuals results ≥ 2.0 or ≤ -2.0

2.3.1 Inclusion and exclusion criteria

For the Intervention group, inclusion criteria were sedentary older adults 60 years or older living in communities with T2DM, ambulatory with or without devices, and able to follow simple exercise instructions without assistance. Additionally, the intervention group must be cleared by their primary physician to perform moderate intensity exercise. The Control group was healthy older adults 60 years or older living in communities who are either sedentary or active and were age- and gender- matched with the intervention group. The inclusion criteria for the sedentary individuals, either healthy (in the Control group) or T2DM (in the Intervention group), was that they perform weekly moderate intensity exercise that is less than 30 minutes a day less than five days a week, except for leisurely walking and light housework based on the Rapid Assessment of Physical Activity [98]. Moderate intensity exercises include, for example, walking faster than usual, aerobics class, cycling, swimming, strength training, swimming, and snow shovelling. For the active Control group of healthy older adults adults 60 years or older living in communities, the additional inclusion criteria

 doi:10.20944/preprints202306.0764.v1

were being able to (1) walk six minutes as quickly as possible without any adverse symptoms including extreme pain on feet or joints, dizziness, vertigo, or nausea; and (2) perform moderate-intensity exercise weekly more than 30 minutes a day five days a week or vigorous physical activities every week more than 20 minutes a day or three days a week. Vigorous physical activities include stair machines, jogging or running, tennis, or badminton. The exclusion criteria were (1) foot deformities, cuts, blisters or amputation, Achilles tendonitis, joint replacements in the past three months, Parkinson's disease, retinopathy such as severe glaucoma, current or uncontrolled vestibular disorders; (2) current cardiopulmonary diseases, vascular diseases, or stroke; (3) dementia indicating the inability to follow exercise instructions independently; (4) blood glucose level above 400 mg/dL or HbA1c > 8.0%, (5) Type 1 diabetes, and (6) local skin fold larger than 40mm that will be detrimental to NIRS. Additional exclusion criteria were (1) current smoking or smoking within the last 12 months; (2) currently receiving or planning to receive physical therapy within two months, and (3) lack of English proficiency.

2.3.2 Recruitment

After approval by the Institutional Review Board of the University at Buffalo, recruitment flyers were sent to senior centres, churches, independent living facilities, assisted living facilities, and the University at Buffalo Clinical and Translational Science Institute, which provided a list of individuals who met the primary inclusion criteria. Some interested individuals contacted the investigator, and for those who did not contact, the investigator either made a phone call or mailed a flyer. We used a consecutive sampling method for the Intervention group. For the Control group, we selected age- and gender- matched participants among the convenience samples. Table 2 shows the cognitive performance where the Intervention group at baseline was found to have mild cognitive impairment when compared to age- and gender- matched participants in the Control group. Figure 1A shows the exercise intervention programme.

Table 2. Cognitive performance comparisons between the participants in the sedentary T2DM Intervention group at baseline and the active and sedentary healthy Control group.

Characteristics	**Intervention group at baseline** **M(SD)**	**Control group** **M(SD)**	**Z**	**Cohen's d**
Mini-Cog	12.79 (2.1)	14.16 (0.9)	Z=3.273** (p=.0005)	d = .967
Trail Making Part A (secs)	39.55 (12.1)	30.94 (6.8)	Z=2.548** (p=.006)	d = .972
Trail Making Part B (secs)	93.45 (26.58)	69.08 (21.3)	Z=3.293***	d = 1.053

Preprints (www.preprints.org) | NOT PEER-REVIEWED | Posted: 12 June 2023 doi:10.20944/preprints202306.0764.v1

			(p<.001)	

* p <.05, ** p<.01, *** p<.001

2.4 Pre- and Post-intervention measurements

2.4.1 Cerebral oxygenation

The fNIRS device used to assess cerebral oxygenation [99] was OctaMon+ (PortaLite, Artinis Medical Systems, The Netherlands), which could measure 8-channels of prefrontal oxyhemoglobin (oxyHb) and deoxyhemoglobin (deoxyHb) at 50 Hz. A headband with two receivers and four high-power transmitters was worn on the forehead for long-separation channels – see Figure 1C. Two low-power transmitters were aligned with the two receivers to measure systemic artefacts in some subjects – see Figure 1C. The fNIRS has established good concurrent validity with functional magnetic resonance imaging (fMRI) and support that fMRI and fNIRS have similar vascular sensitivity based on finger tapping tasks in healthy young ($r=-0.70$, $p<0.001$) and older adults ($r = 0.82$, $p<0.001$) [100],[101]. The prefrontal cortex was measured bilaterally, as shown in Figure 1C, during Mini-Cog.

(A)

Week 1		Week 2		Week 3		Week 4	
Resistance exercise	8 reps	Resistance exercise	8 reps	Resistance exercise	10 reps	Resistance exercise	10 reps
Walking	6 mins	Walking	6 mins	Walking	8 mins	Walking	8 mins
Week 5		**Week 6**		**Week 7**		**Week 8**	
Resistance exercise	12 reps	Resistance exercise	12 reps	Resistance exercise	15 reps	Resistance exercise	15 reps
Walking	10 mins	Walking	10 mins	Walking	12 mins	Walking	12 mins

Preprints (www.preprints.org) | NOT PEER-REVIEWED | Posted: 12 June 2023 doi:10.20944/preprints202306.0764.v1

(B)  (C)

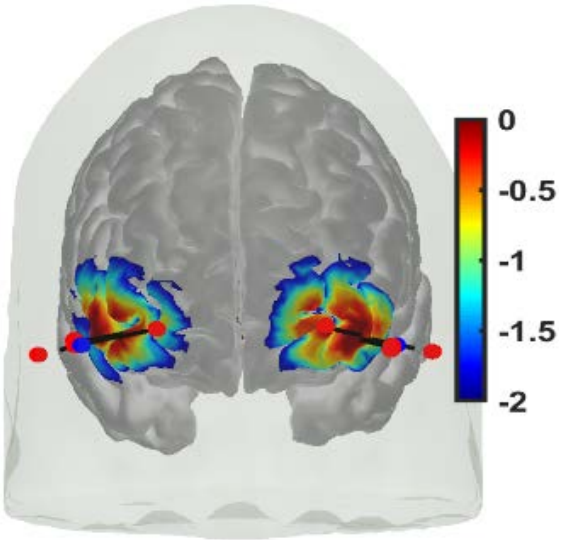

Figure 1: (A) Exercise intervention programme. (B) Pre- and Post-intervention measurements: subject wearing fNIRS headband with two receivers and four transmitters. (B) fNIRS headband optode sensitivity profile (default range of 0.01 to 1 or −2 to 0 in log10 units) with NIR light sources in red and the two detectors in blue.

The headband with fNIRS optodes was attached to the forehead (see Figure 1B). In Figure 1C, optode sensitivity values are displayed logarithmically with a default range of 0.01 to 1 or −2 to 0 in log10 units. The optode montage covered the middle frontal gyrus (orbital part) and the superior frontal gyrus (dorsolateral part) bilaterally (see Figure 1C). Block design is one of the most widely used paradigms in fNIRS experiments that was used in our study. In block design, the same test was repeated several times and the average hemodynamic response was calculated. Here, a block design comprises of repeated blocks of tasks (>=10 sec) and a rest time of usually 10-20 seconds. The rest period allowed the task stimulus-evoked hemodynamic response to return to the baseline. The Mini-Cog has three steps repeated three times and a 10-second rest was given between each step. Data pre-processing was performed using HOMER3 toolbox [102] in Matlab (Mathworks Inc., USA).

 doi:10.20944/preprints202306.0764.v1

A series of offline pre-processing steps were performed in HOMER3 software (https://openfnirs.org/software/homer/), as presented next. The processing stream was made up of five functions. The first function is to convert the raw optical intensity signal into optical density (function: hmrR_Intensity2OD). The second function is motion artefact detection and correction to eliminate noises due to scalp movements such as frowning or raising eyebrows. The motion artefact was removed using a hybrid method based on a spline interpolation method and Savitzky–Golay filtering (function: hmrR_MotionCorrectSplineSG). The parameters are p of 0.99, FrameSize_sec of 10, and turnon of 1. Then the third function is band-pass filtering (function:hmrR_BandpassFilt:Bandpass_Filter_OpticalDensity). A high-pass filter was set up at the cut-off frequency of 0.01 Hz to remove baseline shifts and low-frequency noise. A low pass filter was set at the cut-off frequency of 0.1Hz to remove high-frequency noises caused by heartbeat, respiratory rate, and instrument noise. Then, the pre-processing was followed by conversion to oxyHb and deoxyHb concentration with partial path length factor (function: hmrR_OD2Conc) of 1.0. The last is computation of the hemodynamic response function (HRF) where we aimed at investigating the shape of the HRF without imposing canonical modelling constraints [103]. In prior work, Jahani and colleagues [93] used the time range of 25 to 50 seconds because in this time range the hemodynamic signal reached steady state. Therefore, we used block average (function: hmrR_BlockAvg: Block_Average_on_Concentration_Data) to determine the hemodynamic response during the stimulation period from the resting state to 60 seconds after the stimulus was administered (trange = [-5, 60]). This function gave an average HRF of three trials for Mini-Cog – see Figure 2. Also, we used AtlasViewer software (https://openfnirs.org/software/homer/) to visualize the cortical activation to facilitate anatomical interpretation of the fNIRS data. Here, cortical activation graphs showed the average prefrontal cortex activation using the HRF at a group level and based on our optode sensitivity profile shown in Figure 1C. Since we did not have subject-specific magnetic resonance imaging to create an individual head model, we used the 'Colin27' digital brain atlas (http://mcx.space/wiki/index.cgi?action=browse&id=MMC/Colin27AtlasMesh&oldid=MMC/CollinsAtlasMesh) for the reconstruction of brain activation images with the default regularization scaling parameter = 0.01. Finally, we used the NIRS Brain AnalyzIR Toolbox [104] for statistical analysis that provided a finite impulse response (FIR) model which allowed an unconstrained deconvolution and estimation of the full hemodynamic response [103]. We used the default pipeline (nirs.modules.default_modules.single_subject with resampling at 0.5Hz to reduce computational load), including AR-IRLS for correcting motion and serially correlated errors [105], for the statistical analysis using FIR basis function (nirs.design.basis.FIR with binwidth=1, nbins=30, isIRF=false).

 doi:10.20944/preprints202306.0764.v1

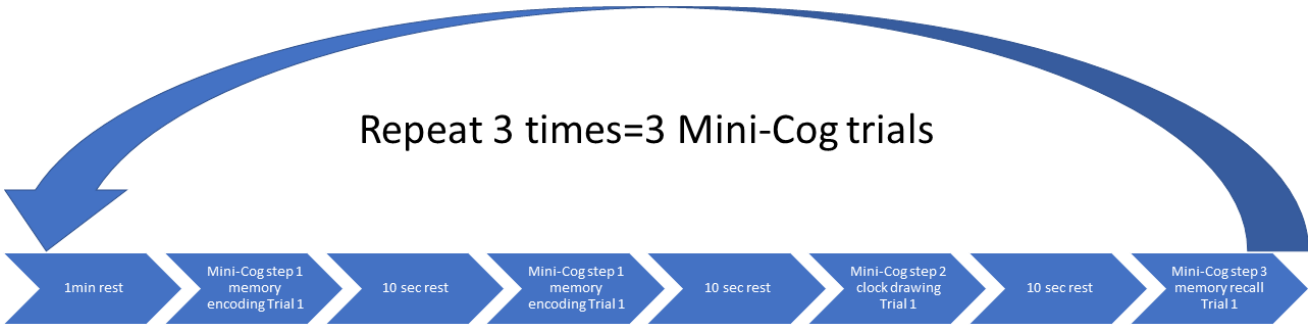

Figure 2: Block Design for the cognitive tasks – Mini-Cog

We also performed operational modal analysis (OMA) on the task stimulus-evoked hemodynamic responses (oxyHb, deoxyHb) where the cognitive load excitation of the prefrontal cortex was considered as realizations of white noise processes. OMA is for the extraction of modal parameters (natural frequency, damping) where we used a covariance-driven Stochastic Subspace Identification (SSI-Cov) approach that also provided modal parameter uncertainty estimates. Here, the principal component analysis provided the projection space for the modal solution [106]. We also used frequency domain decomposition [107] to compare with the SSI-Cov results from time domain decomposition. In our prior computational work on experimental modal analysis (EMA) using multi-modal signals including electroencephalogram [108], we have estimated modal parameters by simple peak picking and found modulation by external excitation with transcranial electrical stimulation (tES). Here, the stabilization diagram for modal analysis (‘modalsd’ in Matlab) allowed selection of stable modes (frequency, damping) that do not change substantially with the change in the size of the model (i.e., estimated number of modes). From our prior computational work on EMA of neurovascular coupling [109],[108],[103], a maximum of 30 modes were estimated in the current study using OMA. Here, we were interested in the physiological modes based on our prior computational work on EMA of neurovascular coupling [109],[108],[103] with frequencies less than 0.2 Hz that were found relevant for fNIRS including low frequency oscillations (LFO) (0.05-0.2 Hz) and very low frequency oscillations (VLFO) (<0.05 Hz) [81],[110]. Finally, we applied a multi-stage clustering for automated OMA built on the definitions of the pole distance and modal assurance criterion (MAC) [111] using the Modal Toolkit (https://code.vt.edu/vibes-lab/modal-analysis).

 doi:10.20944/preprints202306.0764.v1

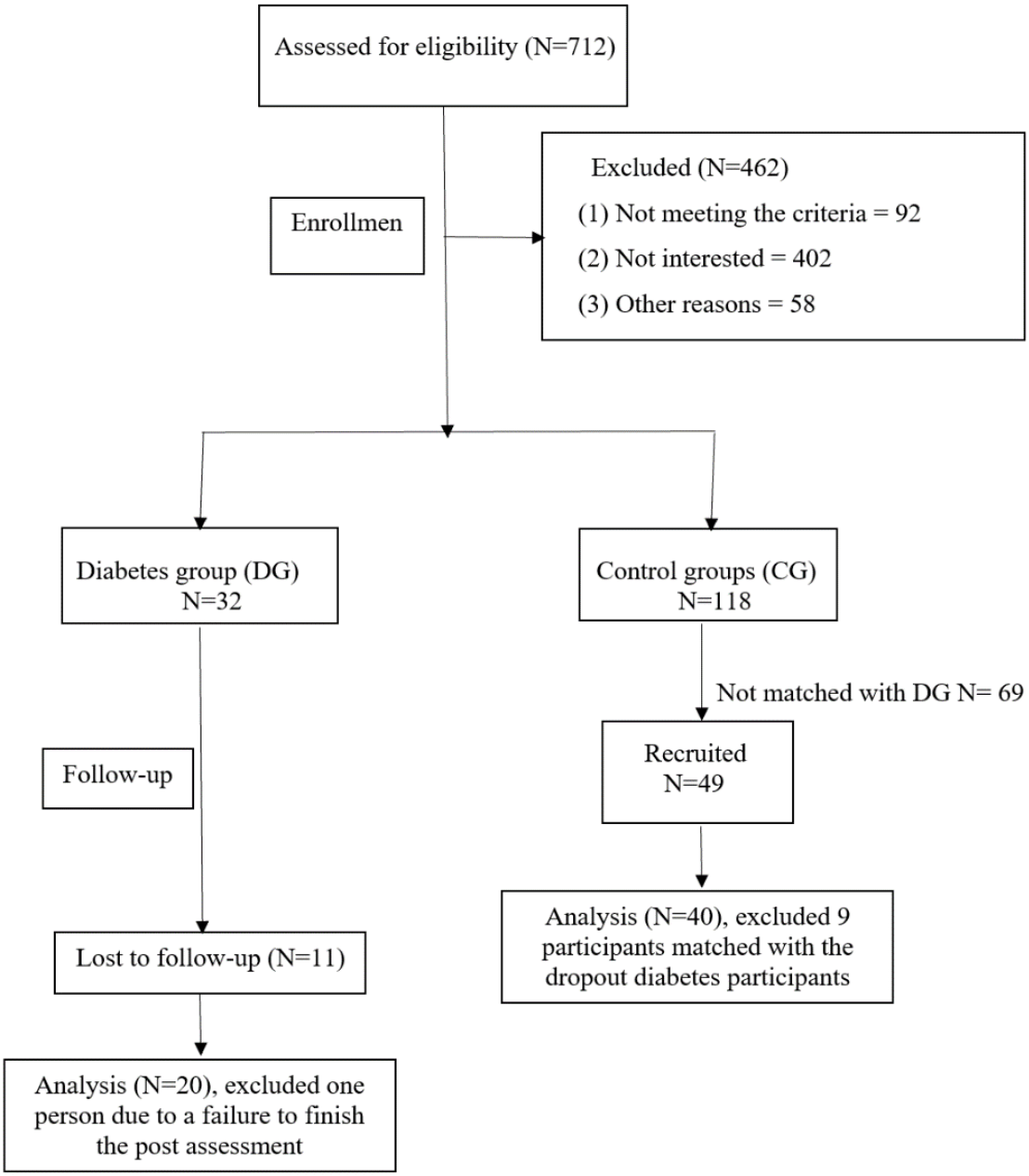

Figure 3: CONSORT flow diagram for screening, eligibility, and included participants.

2.4.2 Muscle oxygenation

We used a wearable device, Moxy 1 (Fortiori Design LLC, Minnesota, USA), which measured SmO2 percentage (%) of the gastrocnemius lateralis muscle at 1 Hz. One band attached to the belly of the calf muscle in the dominant leg of the participants and was secured with the tape. We first located one third along the line from fibular tuberosity to calcaneus tuberosity of the gastrocnemius muscle and attached the muscle sensor at the junction point. The distance from the strap to the lateral malleolus was recorded in each participant to allow reproducible positioning. The validity of muscle NIRS in the exercising muscles has been established to measure SmO2 at low to moderate exercise intensities [112]. Here, SmO2 measured by the Moxy device in the vastus lateralis during cycling showed a very high

 doi:10.20944/preprints202306.0764.v1

correlation between trials (Spearman's order rank coefficient: r = 0.842–0.993), and an intraclass correlation was also high (r = 0.773–0.992, p <.01). It was also highly correlated with oxygen uptake and heart rate (r = 0.71–0.73, p ≤ .01) [112].

We measured two muscle oxygenation features, SmO2 drop during a physical task and SmO2 recovery speed after the physical task [61]. The drop in SmO2 was defined as the difference between the maximum and minimum SmO2 during the physical tasks, the bilateral heel raise (BHR) and the 6 Minute Walk Test (6MWT). Then, SmO2 recovery starts immediately after the participant finishes the physical tasks and sits down. The SmO2 level increases when the recovery period begins. Some participants' SmO2 reaches the maximum during the recovery period and stays stable after that. To calculate SmO2 recovery speed, the first step was to use the maximum SmO2 during recovery to subtract the SmO2 level at the beginning of the recovery period. Then, the difference in SmO2 is divided by the time taken from the beginning to the maximum (seconds), which is the recovery speed (SmO2% per sec) [61].

2.4.3 Cognitive and physical function tests

The Mini-Cog examined cognition while the physical performance was measured using the 6-Minute Walking Test (6MWT) and the Bilateral Heel-Rise (BHR) test. The Mini-Cog instrument assesses short-term memory and visuo-constructive abilities. There are three steps [113], see Figure 2, where the first step is to measure the ability to repeat three words immediately after the experimenter. The second step is to draw a clock based on the verbally assigned time in 3 minutes. The last step is to recall the three words from the first step. Higher scores indicate high levels of cognition and a cut-off point of less than 3 indicates dementia [113]. A systematic review has revealed that the Mini-Cog test has an excellent sensitivity of 0.91 and an excellent specificity of 0.86 to detect dementia [114].

The 6MWT was developed for the measurement of aerobic capacity based on the maximum distance that individuals can walk in 6 minutes [115]. Assistive devices or bracing are allowed to be used and documented. It has good to excellent test-retest reliability (ICC ≥ 0.76) [116]. The BHR test evaluates the endurance performance of the calf muscle, the triceps surae [117], and is performed in a standing position. Participants must stand barefoot, use the dominant hand on the wall to support themselves, and keep the elbow semi-flexed. First, participants do a full range of plantarflexion, and the examiner marks the maximum height at the participant's head on the wall. Then, a marker is placed at the maximum height. After that, participants perform a full range plantarflexion repetitively as fast as possible, and their heads are supposed to touch the marker with each repetition. The maximum number of plantarflexions and the time taken to voluntary fatigue were recorded.

2.5 Protocol

The research proposal was approved by the Institutional Review Board of the University at Buffalo, USA. For the recruitment, a phone screening was conducted based on the inclusion and exclusion criteria once the participants contacted the investigator. After the written consent, assessments were made in the same order for all participants and specific

 doi:10.20944/preprints202306.0764.v1

instructions for the exercise program were provided. For the assessments, first, we made an appointment for participants to visit a University at Buffalo clinical laboratory. After the participants arrived, we explained the study using a consent form. After obtaining the written consent of a participant, we asked the person to test the blood sugar level if it was not measured on that day. After checking that blood glucose is less than 400 mg/dL, to continue the assessment, we measured participants' blood pressure and heart rate for safety considerations. HbA1c and body fat were also measured. Subsequently, demographic and health information were obtained. After collecting basic questions, recording devices were attached – first, we placed a fNIRS device on a participant's forehead to measure cerebral oxyHb. The Mini-Cog was performed three times with three different steps. Each time, there were three Mini-Cog steps: (1) memorizing three words, (2) drawing a clock following given instructions, and (3) recalling three words given in first step. When the tests were completed, the fNIRS device was removed. Participants were asked to drink water if necessary. Then, the muscle NIRS device was placed on the gastrocnemius lateralis. BHR was the first assessment and then rest until SmO2 recovered to the resting level (3 minutes break). Then, the 6MWT was performed, followed by the rest until SmO2 recovered. Finally, blood pressure, heart rate, fatigue, and blood glucose were measured again to ensure that the participants were doing good. Then, we offered water and food containing glucose. The entire assessment took about 2.5 hours per person at each visit for baseline measures and for follow-up. After the assessments, the instructions for the 2-month home exercise were explained to the Intervention group and printed materials were provided. In addition, a pedometer was provided to wear while walking. The investigators conducted a home safety assessment to ensure that the home environment was safe for exercise. After each assessment, $50 was given to each Intervention group participant at the baseline as well as at the follow-up visits, while $40 was given to each Control group participant. The Intervention group participants received biweekly reminder phone calls and were asked to fill out an exercise log every time they exercised. We monitored the adherence rate that is the proportion of prescribed exercises taken.

2.6 Statistical analysis

Wilcoxon rank sum test is a nonparametric test that was performed on the SmO2 drop and the SmO2 recovery speed. The statistical analyses were performed in the software SPSS 28.0. For cerebral oximetry, we applied second-level group statistical models using the NIRS Brain AnalyzIR Toolbox [104] where first an n-way ANOVA using factors, groups (active healthy, sedentary healthy, sedentary T2DM pre, sedentary T2DM post) and conditions (Mini-Cog step1, step2, step3), was applied (‘nirs.modules.AnovaN’ using the NIRS Brain AnalyzIR Toolbox). Then, we applied n-way ANOVA using factors, groups (sedentary T2DM pre, sedentary T2DM post) and conditions (Mini-Cog step1, step2, step3). The significance level was set at 0.05.

3 Results

 doi:10.20944/preprints202306.0764.v1

The mean score of the adherence rate for the 21 participants in the Intervention group who adhered to the 2-month exercise was 89.14% (SD=21.23). The exercise programme included regular biweekly phone calls that helped with the adherence. Figure 4A and 4B show the change in the SmO2 (%) drop in the Intervention group participants (DG in Figure 4) for bilateral heel rise task (BHR, Figure 4A) and the 6-minute walk task (6MWT, Figure 4B) that significantly (α=0.05) changed at follow-up after the 2-month exercise programme from the pre-intervention baseline. In fact, SmO2 (%) drop got better than the sedentary healthy group (SHG in Figure 4) for the BHR. Also, SmO2 (%) drop got better than the active healthy group (AHG in Figure 4) as well as SHG for 6MWT. The SmO2 recovery speed also improved after 2-month exercise programme from the pre-intervention baseline, as shown in Figure 4C and 4D, but did not reach statistical significance (α=0.05). Table 3 shows the SPSS 28.0 test results.

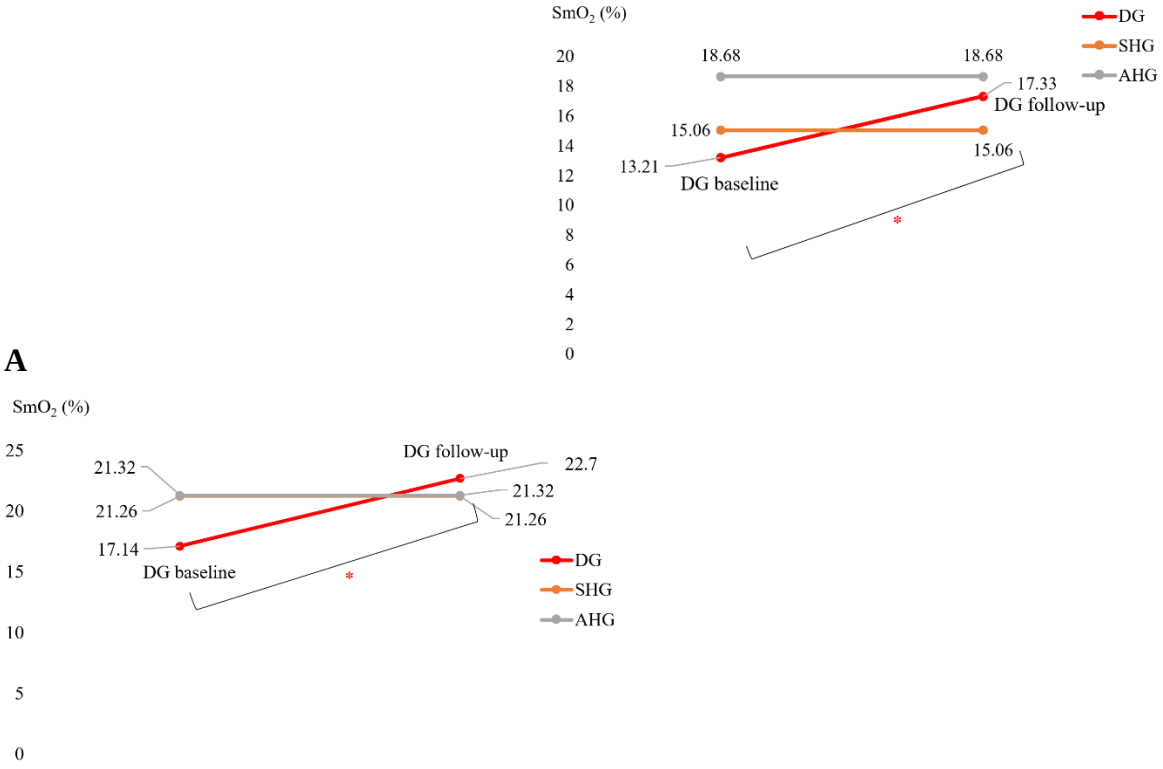

Preprints (www.preprints.org) | NOT PEER-REVIEWED | Posted: 12 June 2023 doi:10.20944/preprints202306.0764.v1

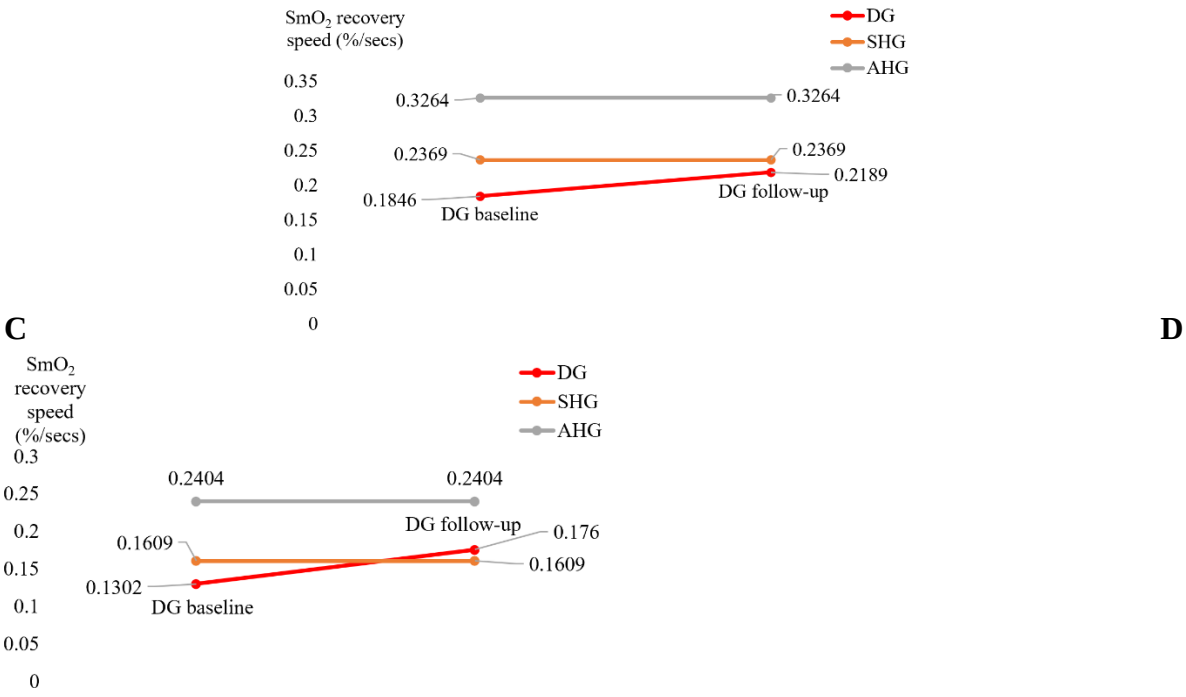

Figure 4. A. SmO2 drop during the BHR test comparisons. B. SmO2 drop during the 6MWT test comparisons. C. BHR SmO2 recovery speed comparisons. D. 6MWT SmO2 recovery speed comparisons.

Table 3. Muscle oxygenation changes during bilateral heel rise task (BHR) and the 6-minute walk task (6MWT) in the sedentary T2DM Intervention group at pre-intervention baseline and post-intervention follow-up.

Characteristics	Baseline M(SD)	Follow-up M(SD)	t or Z	Cohen's d
SmO_2 drop during BHR test (%)	13.21 (7.5)	17.33 (11.6)	t=2.185* (p=.022)	d = -0.515
SmO_2 drop during 6MWT (%)	17.14 (9.1)	22.70 (15.4)	t=1.845* (p=.041)	d = -0.435
BHR SmO_2 recovery speed (%/sec)	.1846 (.071)	.2189 (.107)	t=1.714 (p=.052)	d = -0.404
6MWT SmO_2 recovery speed (%/sec)	.1302(.087)	.1760 (.174)	t=1.094 (p=.145)	d = -0.258

*p <.05, ** p<.01, ***p<.001

Figures 5 to 8 show the prefrontal activation (oxyHb in A and deoxyHb in B) from AtlasViewer software based on the HRFs during Mini-Cog tasks (Mini-Cog step 1 in A1, B1, Mini-Cog step 2 in A2, B2, Mini-Cog step 3 in A3, B3). All the HRFs are presented in the supplementary materials (Figure S1). Here, Figure 5 shows the results from sedentary healthy Control group that showed bilateral Superior frontal gyrus, dorsolateral, oxyHb and deoxyHb activation during memory encoding and clock drawing tasks while only left Superior frontal gyrus, dorsolateral, oxyHb activation and right Superior frontal gyrus,

Preprints (www.preprints.org) | NOT PEER-REVIEWED | Posted: 12 June 2023 doi:10.20944/preprints202306.0764.v1

dorsolateral, oxyHb inactivation during memory recall task. Then, Figure 6 shows the results from active healthy Control group that showed bilateral Superior frontal gyrus, dorsolateral, deoxyHb activation during memory encoding task and oxyHb activation during clock drawing tasks while bilateral Superior frontal gyrus, dorsolateral, deoxyHb activation and oxyHb inactivation during memory recall task. Here, oxyHb and deoxyHb activation may become positively correlated in the presence of systemic confounds and negative correlation between oxyHb and deoxyHb signals can be a characteristic of neurovascular coupling [118] – see the HRFs in the supplementary materials (Figure S1). Notably, the Superior frontal gyrus, dorsolateral, showed activation that is postulated to contribute to higher cognitive functions and particularly to working memory [119]. In prior works, Jahani et al [93] showed the activation of the dorsolateral prefrontal cortex during memory encoding and recalling.

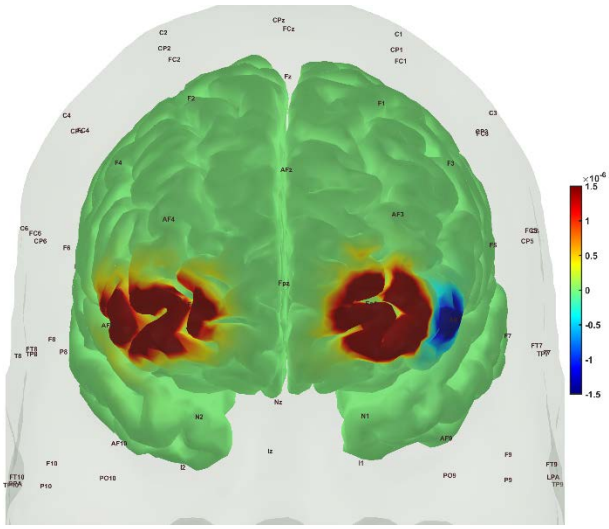

A1 **B1**

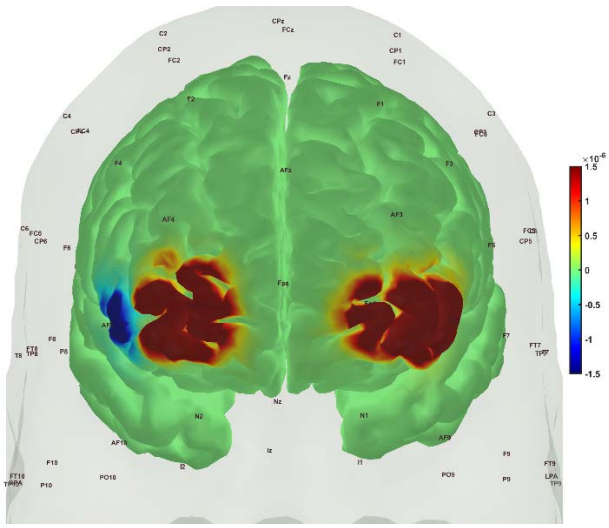

Preprints (www.preprints.org) | NOT PEER-REVIEWED | Posted: 12 June 2023 doi:10.20944/preprints202306.0764.v1

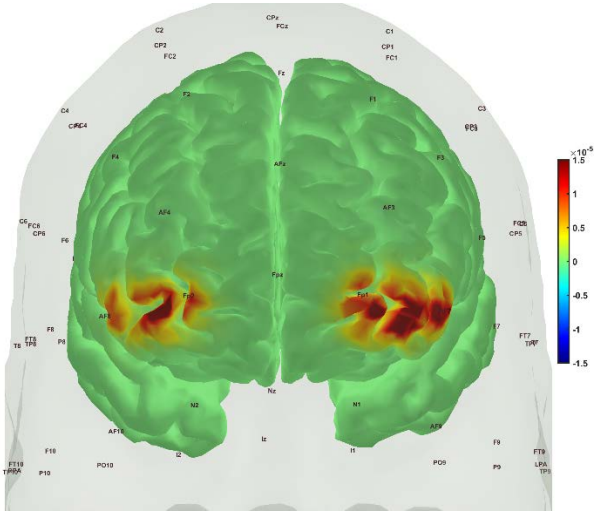

A2 **B2**

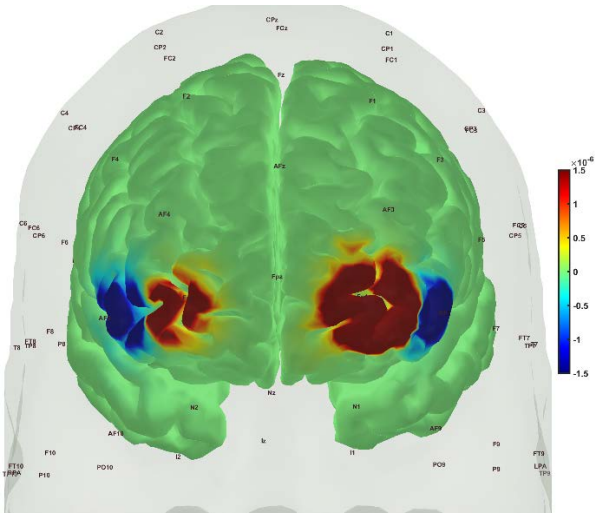

 doi:10.20944/preprints202306.0764.v1

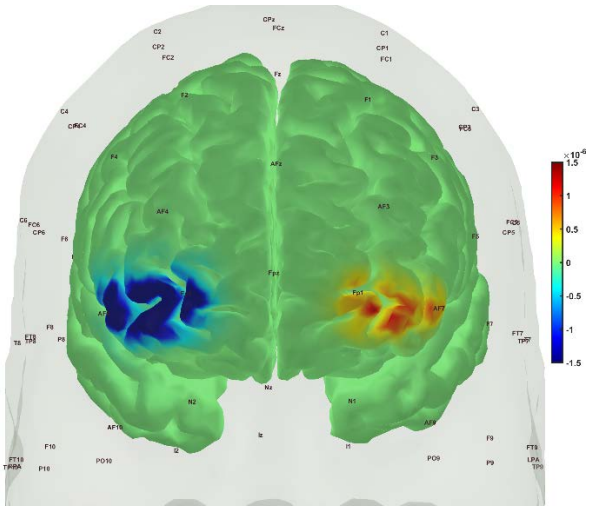

A3 **B3**

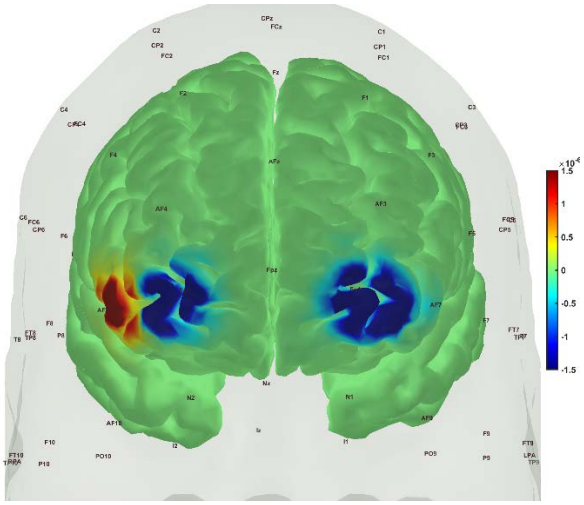

Figure 5. oxyHb (left panels, A1, A2, A3) and deoxyHb (right panels, B1, B2, B3) prefrontal activation in sedentary healthy Control group during A1, B1: Mini-Cog word memory encoding (step 1); A2, B2: Mini-Cog clock drawing (step 2); A3, B3: Mini-Cog word recall (step 3).

Preprints (www.preprints.org) | NOT PEER-REVIEWED | Posted: 12 June 2023 doi:10.20944/preprints202306.0764.v1

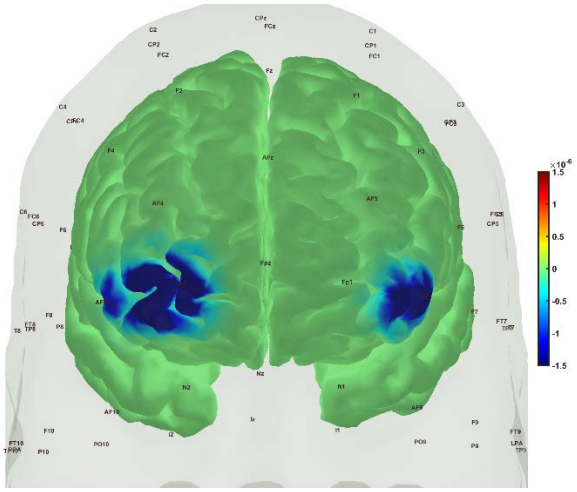

A1 **B1**

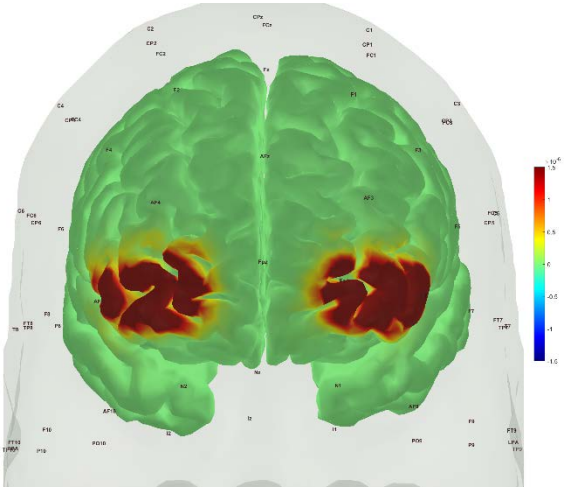

Preprints (www.preprints.org) | NOT PEER-REVIEWED | Posted: 12 June 2023 doi:10.20944/preprints202306.0764.v1

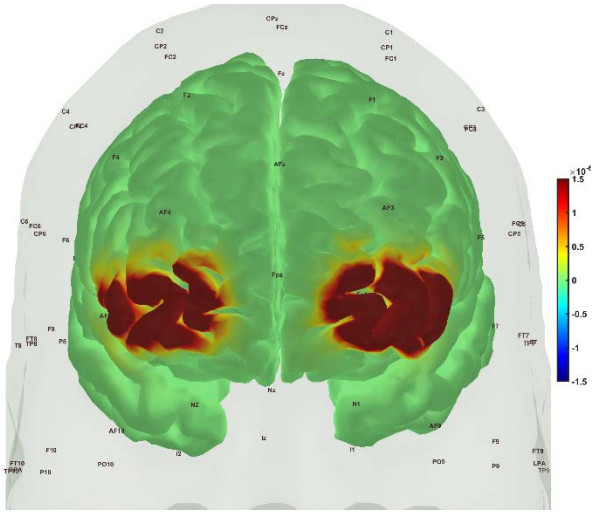

A2 **B2**

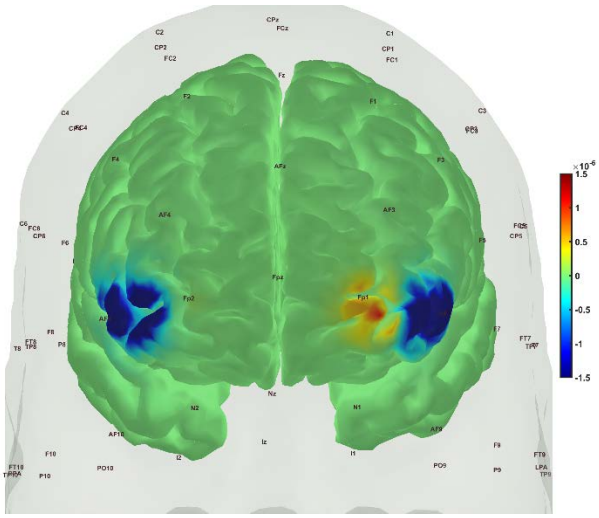

Preprints (www.preprints.org) | NOT PEER-REVIEWED | Posted: 12 June 2023 doi:10.20944/preprints202306.0764.v1

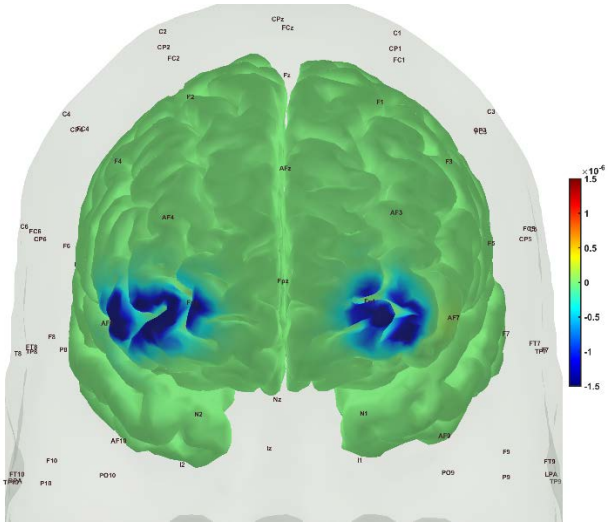

A3 **B3**

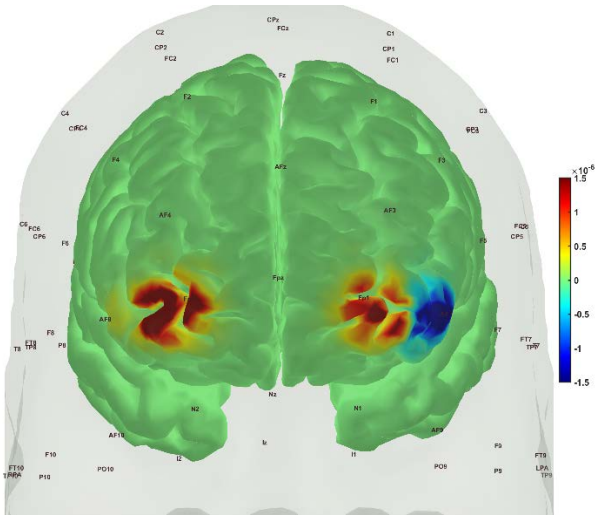

Figure 6. oxyHb (left panels, A1, A2, A3) and deoxyHb (right panels, B1, B2, B3) prefrontal activation in active healthy Control group during A1, B1: Mini-Cog word memory encoding (step 1); A2, B2: Mini-Cog clock drawing (step 2); A3, B3: Mini-Cog word recall (step 3).

In the sedentary T2DM Intervention group, Figure 7 shows primarily negative correlation between oxyHb and deoxyHb activation at the bilateral Superior frontal gyrus, dorsolateral, at the baseline (pre-intervention) that visibly changed at follow-up (post-intervention), as shown in Figure 8, with more similarity to the Figure 6 for the active healthy Control group. N-way ANOVA in NIRS Brain AnalyzIR Toolbox [104] using factors, groups (active healthy, sedentary healthy, sedentary T2DM pre, sedentary T2DM post) and conditions (Mini-Cog step1, step2, step3), showed statistically significant ($p<0.05$, $q<0.05$) effect of only the groups (active healthy, sedentary healthy, sedentary T2DM pre, sedentary T2DM post) on the prefrontal activation at the AAL regions [120], Frontal_Sup_R and Frontal_Sup_L, based on both oxyHb and deoxyHb changes during Mini-Cog test – see Table 4.

Preprints (www.preprints.org) | NOT PEER-REVIEWED | Posted: 12 June 2023 doi:10.20944/preprints202306.0764.v1

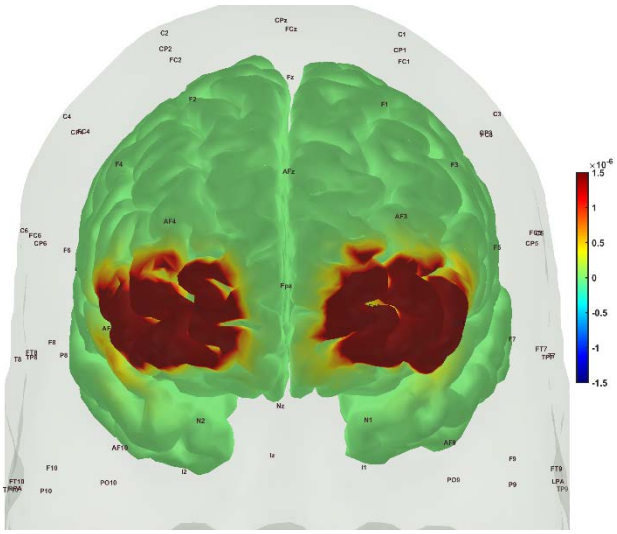

A1 **B1**

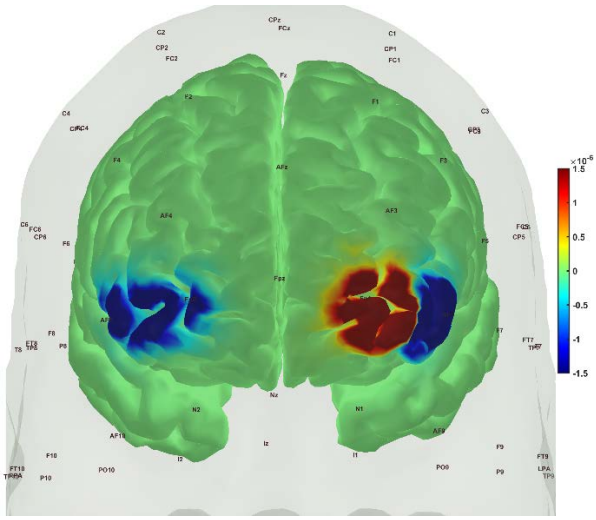

Preprints (www.preprints.org) | NOT PEER-REVIEWED | Posted: 12 June 2023 doi:10.20944/preprints202306.0764.v1

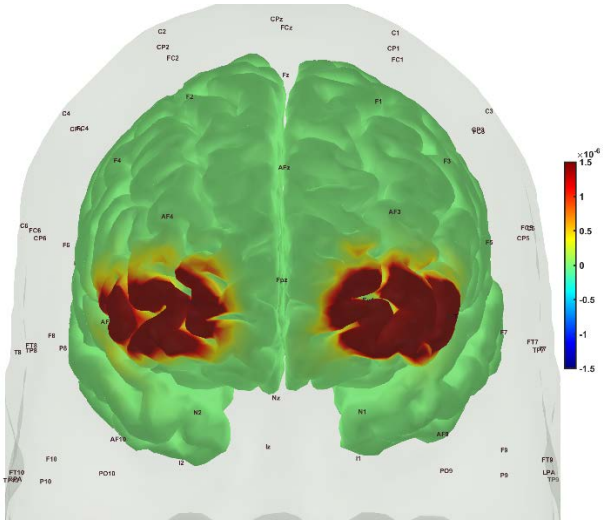

A2 **B2**

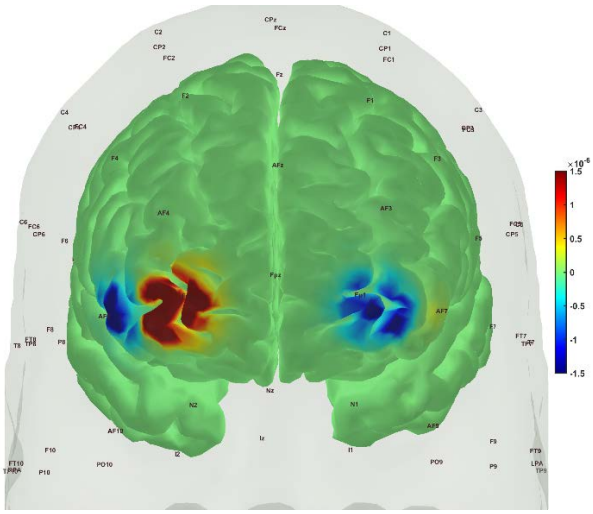

Preprints (www.preprints.org) | NOT PEER-REVIEWED | Posted: 12 June 2023 doi:10.20944/preprints202306.0764.v1

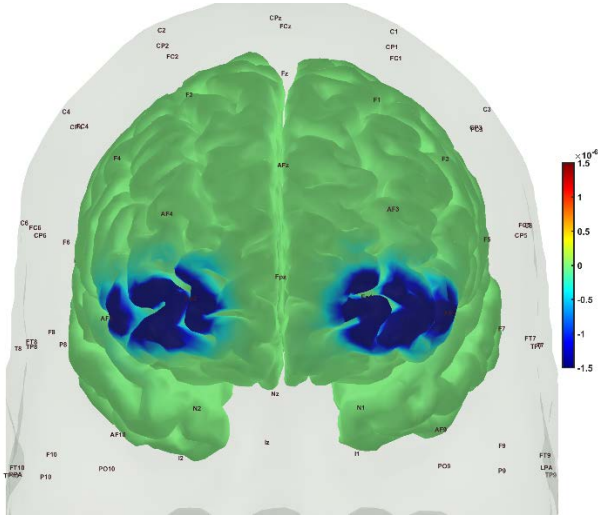

A3 B3

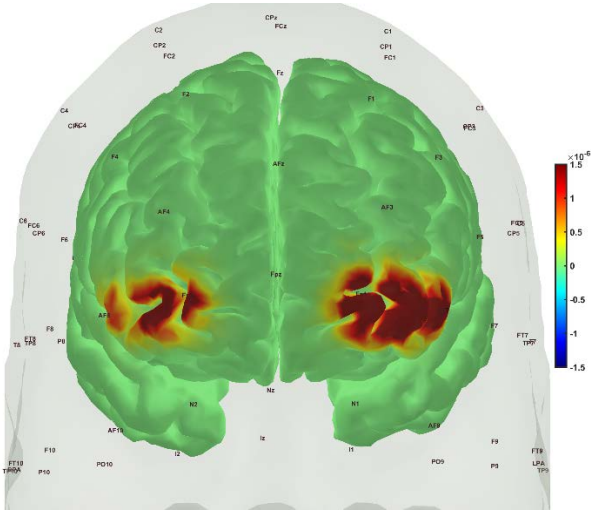

Figure 7. oxyHb (left panels, A1, A2, A3) and deoxyHb (right panels, B1, B2, B3) prefrontal activation in sedentary T2DM Intervention group pre-intervention during A1, B1: Mini-Cog word memory encoding (step 1); A2, B2: Mini-Cog clock drawing (step 2); A3, B3: Mini-Cog word recall (step 3).

Preprints (www.preprints.org) | NOT PEER-REVIEWED | Posted: 12 June 2023 doi:10.20944/preprints202306.0764.v1

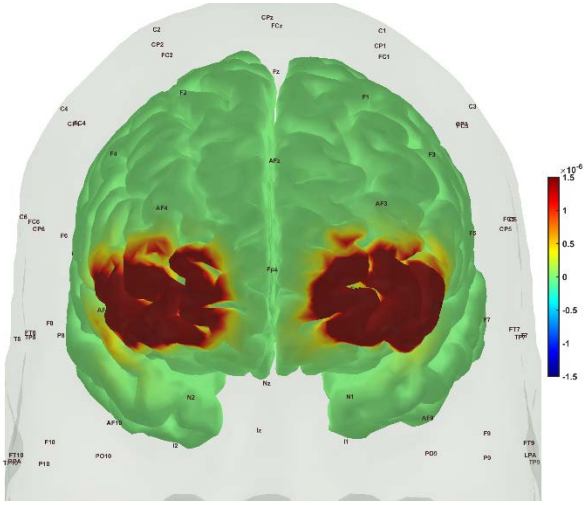

A1 **B1**

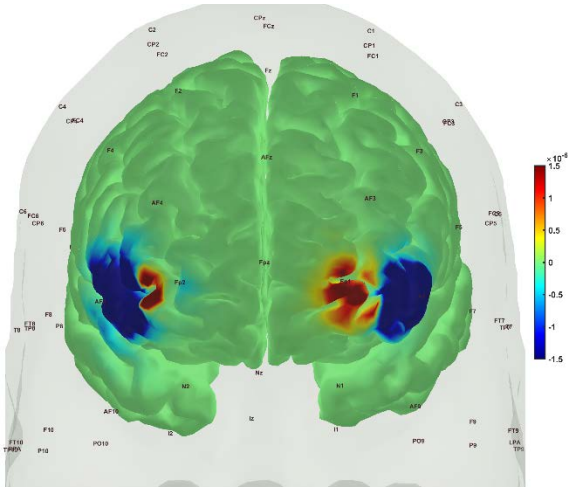

Preprints (www.preprints.org) | NOT PEER-REVIEWED | Posted: 12 June 2023 doi:10.20944/preprints202306.0764.v1

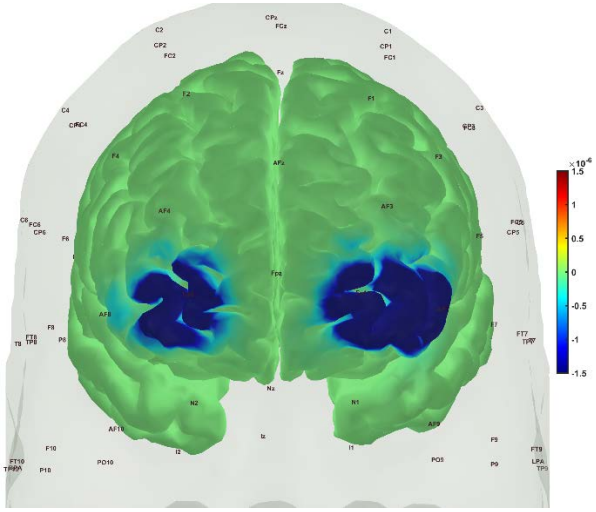

A2 **B2**

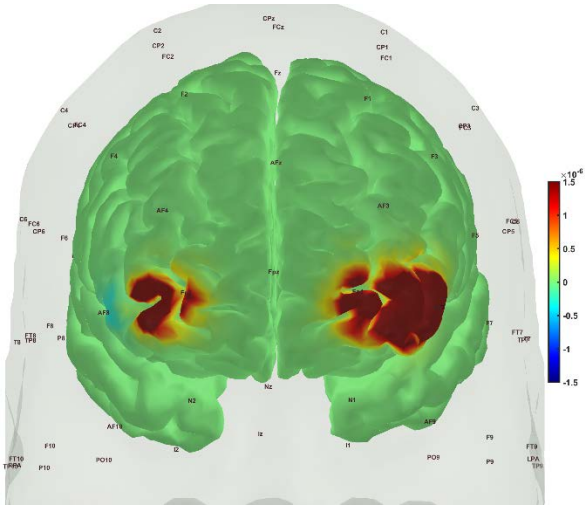

Preprints (www.preprints.org) | NOT PEER-REVIEWED | Posted: 12 June 2023 doi:10.20944/preprints202306.0764.v1

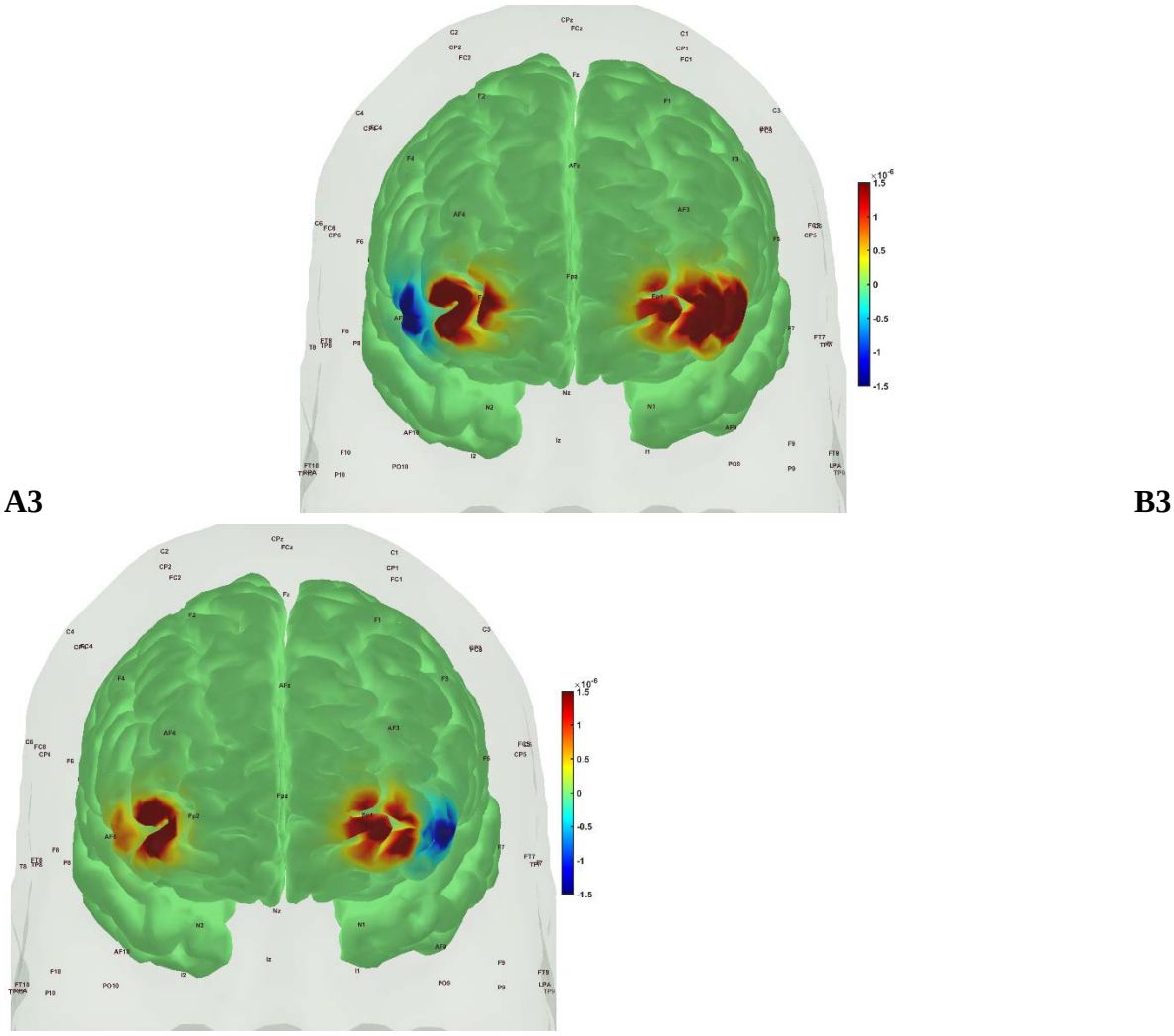

Figure 8. oxyHb (left panels, A1, A2, A3) and deoxyHb (right panels, B1, B2, B3) prefrontal activation in sedentary T2DM Intervention group post-intervention during A1, B1: Mini-Cog word memory encoding (step 1); A2, B2: Mini-Cog clock drawing (step 2); A3, B3: Mini-Cog word recall (step 3).

Table 4: Results from N-way ANOVA in NIRS Brain AnalyzIR Toolbox [104] **using factors, groups (active healthy, sedentary healthy, sedentary T2DM pre, sedentary T2DM post) and conditions (Mini-Cog step1, step2, step3) for the AAL regions** [120] **covered by fNIRS probe.**

AAL region	source	detector	type	factor	p	q
Frontal_Inf_Tri_R	1	1	'hbo'	'cond'	0.999999981	1
Frontal_Inf_Tri_R	1	1	'hbo'	'group'	0.083678248	0.205977227
Frontal_Inf_Tri_R	1	1	'hbr'	'cond'	0.947160368	1
Frontal_Inf_Tri_R	**1**	**1**	**'hbr'**	**'group'**	**0.000314435**	**0.001437418**
Frontal_Sup_R	3	1	'hbo'	'cond'	0.999987864	1
Frontal_Sup_R	**3**	**1**	**'hbo'**	**'group'**	**0.003211619**	**0.012846478**
Frontal_Sup_R	3	1	'hbr'	'cond'	1	1
Frontal_Sup_R	**3**	**1**	**'hbr'**	**'group'**	**1.97E-10**	**3.15E-09**
Frontal_Inf_Tri_L	5	2	'hbo'	'cond'	0.999999039	1
Frontal_Inf_Tri_L	5	2	'hbo'	'group'	0.064006828	0.170684874

Frontal_Inf_Tri_L	5	2	'hbr'	'cond'	0.994658711	1
Frontal_Inf_Tri_L	**5**	**2**	**'hbr'**	**'group'**	**1.82E-05**	**9.70E-05**
Frontal_Sup_L	7	2	'hbo'	'cond'	0.375322014	0.720721989
Frontal_Sup_L	**7**	**2**	**'hbo'**	**'group'**	**6.15E-07**	**4.92E-06**
Frontal_Sup_L	7	2	'hbr'	'cond'	0.999999845	1
Frontal_Sup_L	**7**	**2**	**'hbr'**	**'group'**	**3.44E-06**	**2.20E-05**

BOLD p <.05 and q <.05

Then, investigating the sedentary T2DM Intervention group for post-intervention changes to pre-intervention baseline, N-way ANOVA in NIRS Brain AnalyzIR Toolbox [104] using factors, groups (sedentary T2DM pre, sedentary T2DM post) and conditions (Mini-Cog step1, step2, step3), showed statistically significant ($p<0.05$, $q<0.05$) effect of the groups on the prefrontal activation (both, oxyHb and deoxyHb) at the AAL regions [120], Frontal_Sup_R, during Mini-Cog test – see Table 5. Then, when comparing groups (active healthy, sedentary T2DM post) and conditions (Mini-Cog step1, step2, step3), N-way ANOVA in NIRS Brain AnalyzIR Toolbox [104] showed statistically significant ($p<0.05$, $q<0.05$) effect of the groups on the prefrontal activation at the AAL regions [120], Frontal_Sup_R and Frontal_Inf_Tri_R, based on both oxyHb and deoxyHb changes during Mini-Cog test – see Table 6. Here, Frontal_Sup_R is the Right Superior frontal gyrus, dorsolateral, that is thought to contribute to proactive control of impulsive response [121]; however, the effects of Mini-Cog task-related cerebral (in addition to systemic) autonomic cardiovascular arousal [122] cannot be discounted.

Table 5: Results from N-way ANOVA in NIRS Brain AnalyzIR Toolbox [104] **using factors, groups (sedentary T2DM pre, sedentary T2DM post) and conditions (Mini-Cog step1, step2, step3) for the AAL regions** [120] **covered by fNIRS probe.**

AAL region	source	detector	type	factor	p	q
Frontal_Inf_Tri_R	1	1	'hbo'	'cond'	0.6481	1
Frontal_Inf_Tri_R	**1**	**1**	**'hbo'**	**'group'**	**0.00587**	**0.01879**
Frontal_Inf_Tri_R	1	1	'hbr'	'cond'	0.78319	1
Frontal_Inf_Tri_R	1	1	'hbr'	'group'	0.62103	1
Frontal_Sup_R	3	1	'hbo'	'cond'	0.97924	1
Frontal_Sup_R	**3**	**1**	**'hbo'**	**'group'**	**2.39E-06**	**8.50E-06**
Frontal_Sup_R	3	1	'hbr'	'cond'	1	1
Frontal_Sup_R	**3**	**1**	**'hbr'**	**'group'**	**2.15E-06**	**8.50E-06**
Frontal_Inf_Tri_L	5	2	'hbo'	'cond'	1	1
Frontal_Inf_Tri_L	5	2	'hbo'	'group'	0.7415	1
Frontal_Inf_Tri_L	5	2	'hbr'	'cond'	0.99998	1
Frontal_Inf_Tri_L	5	2	'hbr'	'group'	0.56073	1
Frontal_Sup_L	7	2	'hbo'	'cond'	1	1
Frontal_Sup_L	**7**	**2**	**'hbo'**	**'group'**	**7.59E-08**	**3.47E-07**
Frontal_Sup_L	7	2	'hbr'	'cond'	0.99781	1
Frontal_Sup_L	7	2	'hbr'	'group'	0.56618	1

BOLD p <.05 and q <.05

Preprints (www.preprints.org) | NOT PEER-REVIEWED | Posted: 12 June 2023 doi:10.20944/preprints202306.0764.v1

Table 6: Results from N-way ANOVA in NIRS Brain AnalyzIR Toolbox [104] **using factors, groups (active healthy, sedentary T2DM post) and conditions (Mini-Cog step1, step2, step3) for the AAL regions** [120] **covered by fNIRS probe.**

AAL region	source	detector	type	factor	p	q
Frontal_Inf_Tri_R	1	1	'hbo'	'cond'	0.99999259	1
Frontal_Inf_Tri_R	1	1	'hbo'	'group'	0.056004	0.17322566
Frontal_Inf_Tri_R	1	1	'hbr'	'cond'	1	1
Frontal_Inf_Tri_R	**1**	**1**	**'hbr'**	**'group'**	**0.00543628**	**0.04349027**
Frontal_Sup_R	3	1	'hbo'	'cond'	0.99999952	1
Frontal_Sup_R	3	1	'hbo'	'group'	0.01244236	0.05687937
Frontal_Sup_R	3	1	'hbr'	'cond'	1	1
Frontal_Sup_R	**3**	**1**	**'hbr'**	**'group'**	**8.41E-12**	**1.35E-10**
Frontal_Inf_Tri_L	5	2	'hbo'	'cond'	0.09426186	0.2320292
Frontal_Inf_Tri_L	5	2	'hbo'	'group'	0.06495962	0.17322566
Frontal_Inf_Tri_L	5	2	'hbr'	'cond'	0.97629652	1
Frontal_Inf_Tri_L	5	2	'hbr'	'group'	0.28616516	0.57233033
Frontal_Sup_L	7	2	'hbo'	'cond'	0.01672316	0.06689266
Frontal_Sup_L	7	2	'hbo'	'group'	0.96488565	1
Frontal_Sup_L	7	2	'hbr'	'cond'	1	1
Frontal_Sup_L	7	2	'hbr'	'group'	0.04105912	0.14598797

BOLD p <.05 and q <.05

OMA provided insights where very low frequency oscillations (VLFO) (<0.05 Hz) cluster during Mini-Cog test was missing in the active healthy Control group as well as after 2-month exercise programme in the sedentary T2DM Intervention group – see Figure 9. Here, VLFO (<0.02 Hz) can be endothelial related metabolic [81] and VLFO (>0.02Hz and <0.05 Hz) can be neurogenic sympathetic while low frequency oscillations (LFO) (0.05-0.2 Hz) can be neurovascular coupling and myogenic influences [81],[110].

Preprints (www.preprints.org) | NOT PEER-REVIEWED | Posted: 12 June 2023 doi:10.20944/preprints202306.0764.v1

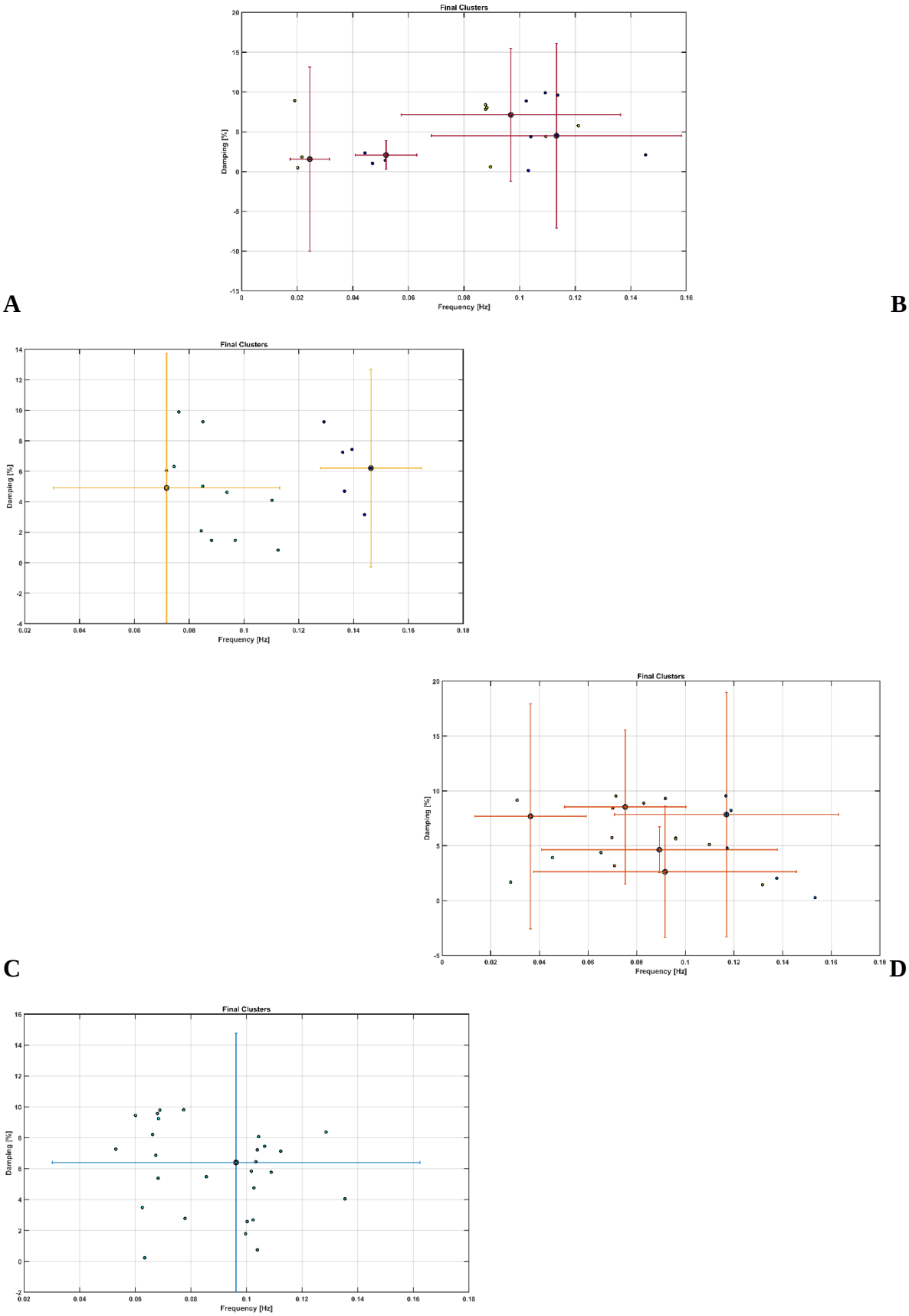

Figure 9. Results from operational modal analysis (OMA) on the task stimulus-evoked hemodynamic responses where the cognitive load excitation of the prefrontal cortex was considered as realizations of the white noise processes. A. sedentary healthy Control

 doi:10.20944/preprints202306.0764.v1

group. B. active healthy Control group. C. sedentary T2DM Intervention group at baseline (pre-intervention). D. sedentary T2DM Intervention group at follow-up (post-intervention).

4 Discussion

Our study showed that the 2-month aerobic and resistance exercise programme influenced the very low frequency oscillations (VLFO) (<0.05 Hz) cluster during Mini-Cog test that was present in the sedentary T2DM Intervention group at baseline (pre-intervention) but was missing after 2-month exercise programme in the sedentary T2DM Intervention group – see Figure 9. The VLFO (>0.02Hz and <0.05 Hz) clusters in the sedentary T2DM Intervention group at baseline (pre-intervention) and the sedentary healthy Control group can be related to vascular muscle and/or perivascular neurogenic regulation when other controls (vasomotor, chemical, and metabolic) become less dominant [123]. This aligns with the postulated Mini-Cog task-related cerebral (in addition to systemic) autonomic cardiovascular arousal [122] due to cognitive load excitation – see also Tables 5 and 6. Also, post-intervention changes to pre-intervention baseline in the sedentary T2DM Intervention group using N-way ANOVA in NIRS Brain AnalyzIR Toolbox [104] showed a statistically significant ($p<0.05$, $q<0.05$) effect of the exercise intervention on the prefrontal activation (both, oxyHb and deoxyHb) at the AAL regions [120], Frontal_Sup_R, during Mini-Cog test – see Table 5. Then, when comparing active healthy and sedentary T2DM post for the conditions (Mini-Cog step1, step2, step3), N-way ANOVA in NIRS Brain AnalyzIR Toolbox [104] showed statistically significant ($p<0.05$, $q<0.05$) effect on the prefrontal activation at the AAL regions [120], Frontal_Sup_R and Frontal_Inf_Tri_R, between the active healthy versus the sedentary T2DM post-intervention groups based on both oxyHb and deoxyHb changes during Mini-Cog test – see Table 6. Here, the effects of Mini-Cog task-related cerebral (in addition to systemic) autonomic cardiovascular arousal [122] cannot be discounted due to our OMA results that indicated an exercise-related effect on VLFO (<0.05 Hz) cluster that can be postulated to be related to vascular muscle and/or perivascular neurogenic regulation [123]. Therefore, we propose that short 2-month aerobic and resistance exercise programme influenced cerebral blood flow regulation via vasomotor, chemical, and metabolic controls that became more dominant [123]. Here, metabolic effect of 2-month aerobic and resistance exercise programme is supported by Table 3 that shows the statistical test results where the significant change in SmO2 (%) drop in the Intervention group participants at follow-up after 2-month exercise programme for BHR and 6MWT tasks was found. In fact, exercise-induced adaptations may include an altered profile of secreted proteins from skeletal muscle and adipose tissue [124] where adiposity in the skeletal muscle may be a risk factor for cognitive decline [125]. So, our study added evidence of impaired oxidative capacity in older adults with T2DM that may be improved with exercise and monitored with muscle oxygenation changes – see Figure S3 in the supplementary materials.

There are prior works on frail older adults and those with mild cognitive impairment and T2DM that support our findings. In the study conducted by Silveira-Rodrigues et al.

 doi:10.20944/preprints202306.0764.v1

[126], 31 sedentary middle-aged and older adults with T2DM were allocated into the combined exercise group three times per week for 8-week or the control group. The 8-week aerobic and resistance exercise training improved working memory and attention/concentration, but not the short-term memory in T2DM participants of the exercise group. Here, the authors [126] concluded that 8-week aerobic and resistance exercise training partially reversed the negative effects of T2DM possibly by the amelioration of metabolic regulation. Another study evaluated a 12-week intervention in 49 middle-aged and older adults with T2DM and found a significant memory improvement [127]. However, unlike these two studies composed of both middle-aged and older adults, all our participants were older adults aged 60 and over. In agreement to Silveira-Rodrigues et al.'s study [126], we found a possible improvement of metabolic regulation of the cerebral blood flow based on our OMA results. A longer duration, for example, 12 weeks intervention may have improved our prefrontal activation results, viz., Leischik et al. [127] study conducted for 12 weeks. Congruent with our results, a previous study found that active older adults tend to have less prefrontal overactivation during motor planning than less active controls indicating possible metabolic and molecular changes induced by physical exercise [128]. Another study compared Kinect-based exergaming with combined exercise training effects in frail older adults [129],[41]. In their study [41], 80% of the participants had normal cognition or mild dementia but not severe dementia. After the 12-week combined exercise, prefrontal overactivation decreased in both the groups during the Montreal Cognitive Assessment or The MoCA Test. As a pioneering study, our clinical trial was conducted on sedentary T2DM participants with mild cognitive impairment when compared to age- and gender- matched participants in the Control group – see Table 2. T2DM increases the risk of developing cognitive impairments where physical exercise can reinforce antioxidative capacity, reduces oxidative stress in T2DM [130]. Here, the decline of cognitive performance in T2DM was proposed to be related to brain tissue impairments, including mitochondrial dysfunction [130], but not well understood yet [131].

A compensation theory has been proposed to explain brain overactivation with ageing and T2DM deficits where Zhang et al. [23] argued that strengthened regional activity in fronto-parietal networks may compensate for the declined working memory (WM) in T2DM subjects. Then, people with mild cognitive impairment (MCI) seems to have abnormal increased medial temporal lobe activation early in the course of prodromal Alzheimer disease (AD) followed by a subsequent decrease as the disease progresses [132]. So, overactivation seems like a compensation strategy in MCI patients to accomplish difficult cognitive tasks. The compensation-related hypothesis states that some brain parts in older adults must work harder than young adults on similar tasks [20] and this deficit seems to be related to gray and white matter atrophy [133]. Apart from the effects of age difference on brain overactivation, the other effect can be due to the nature and complexity of the cognitive tests, leading to overactivation in different regions of the prefrontal cortex. For newly diagnosed middle-aged T2DM subjects, a significant brain overactivation in the right dorsolateral prefrontal cortex, left middle/inferior frontal gyrus, and left parietal cortex were observed in the 2-back test [22]. However, overactivation was not detected during the 0-back and 1-back tests when

 doi:10.20944/preprints202306.0764.v1

compared with healthy controls [22], which indicates that the complexity of the task to evoke cognitive load excitation is important. In our current study, the clock drawing task evoked stronger prefrontal activation than the word memory encoding and recall tasks. The comparison of the two studies indicates that the cognitive task needs to evoke cognitive load excitation which can be achieved better with progressively higher n-back task [22] than Mini-Cog word memorization task used in the current study. Then, the capacity limits may be explained by the limitations on the cellular metabolic energy that can be measured with broadband NIRS [134].

In older adults with T2DM, genes encoding proteins of oxidative metabolism have been shown to be affected, and there were findings of decreased resting mitochondrial activity [135],[136],[137],[138],[139]. So, we postulate that the compensation theory is subserved by hypometabolism, characterized by decreased brain glucose consumption, that is a vicious circle in neurodegenerative diseases [140]. The brain glucose hypometabolism is a prominent feature of AD [141] where it is critical to gain a mechanistic understanding of how the transcranial electrical stimulation (tES) can affect subject's neuroenergetic function underlying cognitive function in early stage AD [142]. In fact, in a large cohort study [143], younger age at onset of diabetes increased the risk of subsequent dementia where AD has been called "type 3 diabetes" due to insulin resistance [144] where mitochondrial dysfunction can be implicated [145]. So, grey-box modeling and causal inference from portable fNIRS measures [146] in response to tES [147] may capture the changes in the neurovascular (including small blood vessels) and neurometabolic (including mitochondria) system [148] in T2DM for model-predictive [149] individualized dosing. Here, we propose spatio-temporal coding [150] based on the dynamical neurovascular assembly framework. Various physiologically relevant frequency bands have already been identified in the literature: 0.6–2 Hz and 0.145–0.6 Hz are related to cardiac and respiratory function, respectively, 0.052–0.145 Hz is associated with smooth muscle cell activity, and 0.021–0.052 Hz may reflect smooth muscle autonomic innervation [151]. Then, in the setting of chronic hyperglycemia, abrupt changes in glycemic control can lead to small fiber neuropathy in patients [152] that may primarily affect 0.021–0.052 Hz oscillations. Then, the low oscillatory frequency (0.01–0.02 Hz) at capillaries is thought to reflect the Fahræus–Lindqvist effect [153], i.e., the nonlinear dependence of apparent blood viscosity on hematocrit and vessel diameter thereby improving endothelial related metabolic interactions [81]. Here, blood viscosity and blood glucose are directly related: blood viscosity is lower in prediabetic subjects than in nondiabetic subjects with blood sugar levels that are high but within the normal range [154]. Then, tES has been shown to reduce blood glucose in men through an insulin-independent mechanism that relates to brain energy metabolism [155]. In addition, cognitive load can significantly reduce blood glucose, such that the amount of cognitive load associated with task performance is an index of its sensitivity to glucose [156]. The first author, Fei Zhao, found a drop in the oscillatory power in the 0.01–0.02-Hz frequency band during the Mini-Cog assessment [157]; this drop was more pronounced in older participants with T2DM than in age-matched subjects that were normoglycemic [158]. Here, a mechanistic understanding of brain energy metabolism is essential vis-a-vis 0.01–0.02 Hz oscillations [153] which may

 doi:10.20944/preprints202306.0764.v1

explain the basis of “diabetic brain fog.” For example, the maximal exercise capacity was found to be positively associated with microvascular glycocalyx thickness at baseline [69] and deteriorated glycocalyx could initiate cardiovascular disease pathology [70]. Also, low transport across blood brain barrier (BBB) [159], including low glucose and insulin [160], can switch the local metabolism from glycolysis to fatty acid oxidation mainly in the astrocytes where women have been found to be at an increased risk [161]. Here, a glial upregulation of fatty acid metabolism to compensate for neuronal glucose hypometabolism in AD has been suggested which correlate with amyloid and tau pathology [161].

Mechanistic investigation of gene-environment interactions can be accomplished by utilizing a subject-specific brain organoid model derived from human-induced pluripotent stem cells (iPSCs), which enables the testing of optical theranostics as demonstrated by Karanth et al. [162]. To delve further into the underlying mechanisms, an in-vitro subject-specific brain organoid model, also described by Karanth et al. [162], can be subjected to oxygen glucose perturbations for detailed mechanistic studies. Notably, our own in-vitro subject-specific brain organoid study [162], accessible at https://neuromodec.org/nyc-neuromodulation-online-2020/P18.html, revealed significant findings of non-invasive brain stimulation. Photobiomodulation led to an increase in cytochrome c oxidase (CCO) activity and pH in the organoid tissue, while simultaneously causing a decrease in the electrophysiological spectral exponent associated with the excitatory-inhibitory (E-I) balance [163]. These preliminary results hold importance for future research on non-pharmacological therapeutics to address the capacity limits of cellular metabolism [134]. In our phase zero studies [164], we employed the brain organoid platform developed by Karanth et al. [162]. This platform can incorporate a dual polymer sensor embedded within the Matrigel matrix, allowing real-time monitoring of glucose and oxygen levels [165] during mitochondrial photobiomodulation. This monitoring can facilitate the investigation of the neurometabolic dose/response relationship, enabling personalized delivery of treatment [166]. However, it is important to note that our current brain organoid model [162] does not replicate neurovascular coupling. The incorporation of vascularized organoids, as suggested by Zhao et al. [167], may provide a viable avenue for studying neurovascular coupling in future investigations. Then, in human studies, we have investigated the transient initial (0–150 s) total hemoglobin response to transcranial direct current stimulation (tDCS) [168] after removing the oscillatory nonlinear calcium dynamics during myogenic smooth muscle activity in the frequency range of 0.05–0.2 Hz, including the ~0.1-Hz hemodynamic oscillations in the fNIRS time series. Here, we investigated very-low-frequency oscillations (0.01 to 0.05 Hz) that can originate from arterioles under autonomic innervation, which is crucial in small vessel function and may be dysfunctional in T2DM. In our study on 19 elderly (60 years and older) with T2DM and 38 age-matched controls [158], we found a significantly lower relative power in 0.021–0.052 Hz frequency band in elderly subjects with T2DM during the Mini-Cog three-item recall test – potentially due to small fiber neuropathy [152]. This is important since diabetic neuropathy is a common complication of diabetes affecting approximately 50% of diabetic patients [169]. Then, ~0.1-Hz hemodynamic oscillations can be related to the synchronization of the intermittent release of calcium within vascular mural cells, including smooth muscle cells (SMCs), where contractile mural cells

 doi:10.20944/preprints202306.0764.v1

are known to generate spontaneous calcium transients. Investigation of coupled steady-state vessel oscillations in low-frequency (≤0.1 Hz) range coupled with electroencephalogram (EEG) band power [170] in patients with early-stage AD with and without T2DM can be motivated by prior works that found a cross-correlation between log (base 10)-transformed EEG band power (0.5–11.25 Hz) and fNIRS O2Hb signals in that low-frequency (≤0.1 Hz) range. Then, longer duration (>3min with 1mA [171]) tDCS application can have polarity specific effects [172] that modulate the cortical excitability likely by the potassium (K+) ions [173],[174] that are released and accumulate in the vicinity of capillaries, then sensed by the capillary network with the inwardly rectifying K+ channel Kir acting as the sensor, which can then modulate the neurovascular system's sensitivity [168],[175]. Also, longer-duration tDCS, postulated to elevate extracellular K+, can decrease calcium activity mediated by the inward-rectifying potassium (Kir) channel in mural cells [175]. Besides Kir channels, voltage-dependent potassium channels, calcium-activated potassium channels, and ATP-activated potassium channels are also present in the mural cells and can interact with the dilatory stress-induced calcium transients. Here, tES effects on the contractile mural cells that encircle the precapillary sphincter [176] at the transition between the penetrating arteriole and the first-order capillary may be crucial for intracerebral microcapillary modulation [177]. Then, tDCS modulated brain activity and neuronal glucose metabolism are also linked [178] for longer duration (>3min with 1mA [171]) tDCS application. Here, longer-term tDCS can lead to the accumulation of local metabolites that can influence cerebral blood flow regulation via changes in the vasomotor, chemical, and metabolic controls [103,123]. We postulate that the subject-specific tES dose-response can be captured by the neurovascular (between the hemodynamic fNIRS signal with the EEG band power) and neurometabolic (between the CCO fNIRS signal with the EEG band power) coupling for model predictive control of tES [150],[166]. Here, a physiologically detailed neurovascular coupling model [168], showed that all pathways in the neurovascular unit evoked steady-state vessel oscillations, which is expected from the experimental literature [179]. Moreover, the EEG band power oscillations and the vasomotion can entrain each other [179], including facilitating paravascular clearance [180], that may be modulated by model predictive control of tES [170],[166]. Then, the model predictive control effects can be elucidated with multimodal imaging [181] in 3D cultured brain organoids [182], and human model for system identification [176],[183] in future works.

This study has several limitations as well as strengths. One limitation is the study design, as it lacked a true control group of individuals with T2DM without any intervention. This was due to time constraints, funding shortages, and the ongoing COVID-19 pandemic. Instead, the study compared T2DM participants with healthy controls measured once, assuming that the controls remained unchanged within two months. However, if the healthy controls had been measured twice during the COVID-19 pandemic, their physical activity levels would likely have declined, potentially biasing the outcomes in favor of the study. The study also lacked participants in the physically active category, limiting the analysis controlling for physical activity levels. Another limitation relates to the self-reporting of diet. Although most participants reported no changes in their diet, the accuracy of self-reporting was not verified. This is important because diet can impact insulin control, which is relevant

 doi:10.20944/preprints202306.0764.v1

to the study's objectives. The third limitation is the high dropout rate of 34.7%. Various reasons accounted for the dropout, including injuries, failed screenings, COVID-19 infections, health issues, personal schedule changes, and family reasons. The high dropout rate resulted in a small sample size, which may have increased the likelihood of Type II errors (failure to find a difference when one exists) and reduced statistical power. Additionally, the study lacked a follow-up with participants after the two-month exercise intervention, which could have provided valuable insights into adherence to the exercise program and its long-term effectiveness. It would have been beneficial to explore the participants' ability to continue and perform high-intensity exercise after improving their activity levels and performance. Another challenge faced during the study was eliminating systemic noise from recorded data due to unavailability of short separation channel measures in all the subjects. So, we verified the negative correlation between oxyHb and deoxyHb signals as a characteristic of neurovascular coupling – see the HRFs in the supplementary materials (Figure S1).

Despite these limitations, the study has strengths. The completion rate for the 2-month exercise program was high, with participants completing an average of 89.14% of exercise sessions. This indicates that the exercise program was practical, doable, and well-tolerated, even during the pandemic. The program was safe, required minimal equipment (ankle weights), and did not require supervision. The exercise instructions were easy to understand, making them suitable for older adults with cognitive decline. The study provided innovative evidence on brain overactivation among older adults with T2DM, supporting the compensatory theory. It demonstrated that the 2-month combined exercise intervention effectively reduced brain overactivation and contributed to improved cognitive function. Here, OMA results indicated an exercise-related effect on VLFO (<0.05 Hz) cluster that can be postulated to be related to better vascular muscle and/or perivascular neurogenic regulation. Furthermore, the study personalized exercise duration and interval based on muscle oxygenation during physical tasks, leading to improvements in muscle oxidative capacity in just two months. This finding has clinical implications for physical therapists, as targeting muscle oxygenation changes during physical tests and utilizing the information to prescribe proper exercise dose that can enhance physical performance. Indeed, adiposity accumulating in the skeletal muscle may be an important risk factor for cognitive decline.

In summary, this study had limitations in terms of study design, lack of control group, limited analysis of physical activity levels, self-reporting of diet without verification, high dropout rate, and absence of follow-up. However, it also demonstrated practicality and effectiveness of our 2-month exercise program, provided valuable insights into brain and muscle response to the 2-month exercise program, and offered personalized exercise recommendations that can be based on muscle oxygenation changes in the future studies.

Conflict of Interest

The authors declare that the research was conducted in the absence of commercial or financial relationships that could be construed as a potential conflict of interest.

Authors' Contributions

F.Z.: conduction of the clinical trial and data curation, formal analysis, investigation, methodology, software application, validation, visualization, writing—original draft. M.T.: conceptualization of the clinical trial, methodology, project administration, resources, supervision, validation, writing—original draft, review. A.D.: conceptualization of the portable imaging and computational methods and data analysis, formal analysis, investigation, methodology, project administration, resources, supervision, validation, visualization, writing—original draft, review and editing. all authors have read and agreed to the published version of the manuscript.

Funding

Portable imaging device testing, validation, and computational data analysis was conducted at the Neuroengineering and Informatics for Rehabilitation Laboratory while the clinical trial was conducted at the Department of Rehabilitation Science, University at Buffalo, and was funded by the Community for Global Health Equity at the University at Buffalo, USA (Anirban Dutta), Buffalo Blue Sky program (Machiko Tomita) and student fellowship (Fei Zhao). The funders had no role in the study design, data collection and analysis, decision to publish, or preparation of the manuscript.

Acknowledgments

The authors acknowledge the Community for Global Health Equity project collaborators, Prof. Lahiri, and Dr. Das (https://www.nature.com/articles/nindia.2019.172).

Data Availability Statement

The human data that support the findings of this study are available upon reasonable request. Due to privacy and ethical restrictions, the raw data cannot be publicly shared. However, interested researchers can contact the corresponding author to request access to the de-identified dataset for the purpose of further analysis and replication of the results.

References

1. Vos, T.; Lim, S.S.; Abbafati, C.; Abbas, K.M.; Abbasi, M.; Abbasifard, M.; Abbasi-Kangevari, M.; Abbastabar, H.; Abd-Allah, F.; Abdelalim, A.; et al. Global Burden of 369 Diseases and Injuries in 204 Countries and Territories, 1990–2019: A Systematic Analysis for the Global Burden of Disease Study 2019. *The Lancet* **2020**, *396*, 1204–1222, doi:10.1016/S0140-6736(20)30925-9.
2. Meisl, G.; Hidari, E.; Allinson, K.; Rittman, T.; DeVos, S.L.; Sanchez, J.S.; Xu, C.K.; Duff, K.E.; Johnson, K.A.; Rowe, J.B.; et al. In Vivo Rate-Determining Steps of Tau

Seed Accumulation in Alzheimer's Disease. *Sci Adv* **2021**, *7*, eabh1448, doi:10.1126/sciadv.abh1448.

3. Standards of Medical Care in Diabetes—2016 Abridged for Primary Care Providers. *Clin Diabetes* **2016**, *34*, 3–21, doi:10.2337/diaclin.34.1.3.
4. Zhao, G.; Ford, E.S.; Li, C.; Balluz, L.S. Physical Activity in U.S. Older Adults with Diabetes Mellitus: Prevalence and Correlates of Meeting Physical Activity Recommendations. *J Am Geriatr Soc* **2011**, *59*, 132–137, doi:10.1111/j.1532-5415.2010.03236.x.
5. Cuff, D.J.; Meneilly, G.S.; Martin, A.; Ignaszewski, A.; Tildesley, H.D.; Frohlich, J.J. Effective Exercise Modality to Reduce Insulin Resistance in Women with Type 2 Diabetes. *Diabetes Care* **2003**, *26*, 2977–2982, doi:10.2337/diacare.26.11.2977.
6. Hamasaki, H. Daily Physical Activity and Type 2 Diabetes: A Review. *World J Diabetes* **2016**, *7*, 243–251, doi:10.4239/wjd.v7.i12.243.
7. Özdirenç, M.; Biberoğlu, S.; Özcan, A. Evaluation of Physical Fitness in Patients with Type 2 Diabetes Mellitus. *Diabetes Research and Clinical Practice* **2003**, *60*, 171–176, doi:10.1016/S0168-8227(03)00064-0.
8. Advika, T.S.; Idiculla, J.; Kumari, S.J. Exercise in Patients with Type 2 Diabetes: Facilitators and Barriers - A Qualitative Study. *J Family Med Prim Care* **2017**, *6*, 288–292, doi:10.4103/2249-4863.219998.
9. Fagour, C.; Gonzalez, C.; Pezzino, S.; Florenty, S.; Rosette-Narece, M.; Gin, H.; Rigalleau, V. Low Physical Activity in Patients with Type 2 Diabetes: The Role of Obesity. *Diabetes Metab* **2013**, *39*, 85–87, doi:10.1016/j.diabet.2012.09.003.
10. Hamilton, M.T.; Hamilton, D.G.; Zderic, T.W. Sedentary Behavior as a Mediator of Type 2 Diabetes. *Med Sport Sci* **2014**, *60*, 11–26, doi:10.1159/000357332.
11. Abd El-Kader, S.M.; Al-Jiffri, O.H.; Al-Shreef, F.M. Aerobic Exercises Alleviate Symptoms of Fatigue Related to Inflammatory Cytokines in Obese Patients with Type 2 Diabetes. *Afr Health Sci* **2015**, *15*, 1142–1148, doi:10.4314/ahs.v15i4.13.
12. Toledo, F.G.S.; Menshikova, E.V.; Azuma, K.; Radiková, Z.; Kelley, C.A.; Ritov, V.B.; Kelley, D.E. Mitochondrial Capacity in Skeletal Muscle Is Not Stimulated by Weight Loss despite Increases in Insulin Action and Decreases in Intramyocellular Lipid Content. *Diabetes* **2008**, *57*, 987–994, doi:10.2337/db07-1429.
13. Radaelli, R.; Fleck, S.J.; Leite, T.; Leite, R.D.; Pinto, R.S.; Fernandes, L.; Simão, R. Dose-Response of 1, 3, and 5 Sets of Resistance Exercise on Strength, Local Muscular Endurance, and Hypertrophy. *J Strength Cond Res* **2015**, *29*, 1349–1358, doi:10.1519/JSC.0000000000000758.
14. Schoenfeld, B.J.; Peterson, M.D.; Ogborn, D.; Contreras, B.; Sonmez, G.T. Effects of Low- vs. High-Load Resistance Training on Muscle Strength and Hypertrophy in Well-Trained Men. *J Strength Cond Res* **2015**, *29*, 2954–2963, doi:10.1519/JSC.0000000000000958.

15. Poirier, P.; Garneau, C.; Bogaty, P.; Nadeau, A.; Marois, L.; Brochu, C.; Gingras, C.; Fortin, C.; Jobin, J.; Dumesnil, J.G. Impact of Left Ventricular Diastolic Dysfunction on Maximal Treadmill Performance in Normotensive Subjects with Well-Controlled Type 2 Diabetes Mellitus. *Am J Cardiol* **2000**, *85*, 473–477, doi:10.1016/s0002-9149(99)00774-2.

16. Allen, K.V.; Frier, B.M.; Strachan, M.W.J. The Relationship between Type 2 Diabetes and Cognitive Dysfunction: Longitudinal Studies and Their Methodological Limitations. *Eur J Pharmacol* **2004**, *490*, 169–175, doi:10.1016/j.ejphar.2004.02.054.

17. Arvanitakis, Z.; Wilson, R.S.; Bienias, J.L.; Evans, D.A.; Bennett, D.A. Diabetes Mellitus and Risk of Alzheimer Disease and Decline in Cognitive Function. *Arch Neurol* **2004**, *61*, 661–666, doi:10.1001/archneur.61.5.661.

18. Cukierman, T.; Gerstein, H.C.; Williamson, J.D. Cognitive Decline and Dementia in Diabetes--Systematic Overview of Prospective Observational Studies. *Diabetologia* **2005**, *48*, 2460–2469, doi:10.1007/s00125-005-0023-4.

19. CHOI, S.E.; ROY, B.; FREEBY, M.; MULLUR, R.; WOO, M.A.; KUMAR, R. Prefrontal Cortex Brain Damage and Glycemic Control in Patients with Type 2 Diabetes. *J Diabetes* **2020**, *12*, 465–473, doi:10.1111/1753-0407.13019.

20. Reuter-Lorenz, P.A.; Cappell, K.A. Neurocognitive Aging and the Compensation Hypothesis. *Curr Dir Psychol Sci* **2008**, *17*, 177–182, doi:10.1111/j.1467-8721.2008.00570.x.

21. Wood, A.G.; Chen, J.; Moran, C.; Phan, T.; Beare, R.; Cooper, K.; Litras, S.; Srikanth, V. Brain Activation during Memory Encoding in Type 2 Diabetes Mellitus: A Discordant Twin Pair Study. *J Diabetes Res* **2016**, *2016*, 3978428, doi:10.1155/2016/3978428.

22. He, X.-S.; Wang, Z.-X.; Zhu, Y.-Z.; Wang, N.; Hu, X.; Zhang, D.-R.; Zhu, D.-F.; Zhou, J.-N. Hyperactivation of Working Memory-Related Brain Circuits in Newly Diagnosed Middle-Aged Type 2 Diabetics. *Acta Diabetol* **2015**, *52*, 133–142, doi:10.1007/s00592-014-0618-7.

23. Zhang, Y.; Lu, S.; Liu, C.; Zhang, H.; Zhou, X.; Ni, C.; Qin, W.; Zhang, Q. Altered Brain Activation and Functional Connectivity in Working Memory Related Networks in Patients with Type 2 Diabetes: An ICA-Based Analysis. *Sci Rep* **2016**, *6*, 23767, doi:10.1038/srep23767.

24. Barloese, M.C.J.; Bauer, C.; Petersen, E.T.; Hansen, C.S.; Madsbad, S.; Siebner, H.R. Neurovascular Coupling in Type 2 Diabetes With Cognitive Decline. A Narrative Review of Neuroimaging Findings and Their Pathophysiological Implications. *Front Endocrinol (Lausanne)* **2022**, *13*, 874007, doi:10.3389/fendo.2022.874007.

25. Sorond, F.A.; Schnyer, D.M.; Serrador, J.M.; Milberg, W.P.; Lipsitz, L.A. Cerebral Blood Flow Regulation during Cognitive Tasks: Effects of Healthy Aging. *Cortex* **2008**, *44*, 179–184, doi:10.1016/j.cortex.2006.01.003.

26. Beishon, L.C.; Hosford, P.; Gurung, D.; Brassard, P.; Minhas, J.S.; Robinson, T.G.; Haunton, V.; Panerai, R.B. The Role of the Autonomic Nervous System in Cerebral Blood Flow Regulation in Dementia: A Review. *Auton Neurosci* **2022**, *240*, 102985, doi:10.1016/j.autneu.2022.102985.

27. Kisler, K.; Nelson, A.R.; Montagne, A.; Zlokovic, B.V. Cerebral Blood Flow Regulation and Neurovascular Dysfunction in Alzheimer Disease. *Nat Rev Neurosci* **2017**, *18*, 419–434, doi:10.1038/nrn.2017.48.

28. Binder, J.R.; Rao, S.M.; Hammeke, T.A.; Frost, J.A.; Bandettini, P.A.; Hyde, J.S. Effects of Stimulus Rate on Signal Response during Functional Magnetic Resonance Imaging of Auditory Cortex. *Cognitive Brain Research* **1994**, *2*, 31–38, doi:10.1016/0926-6410(94)90018-3.

29. Jiang, D.; Lu, H. Cerebral Oxygen Extraction Fraction MRI: Techniques and Applications. *Magnetic Resonance in Medicine* **2022**, *88*, 575–600, doi:10.1002/mrm.29272.

30. Buxton, R.B.; Griffeth, V.E.M.; Simon, A.B.; Moradi, F. Variability of the Coupling of Blood Flow and Oxygen Metabolism Responses in the Brain: A Problem for Interpreting BOLD Studies but Potentially a New Window on the Underlying Neural Activity. *Front Neurosci* **2014**, *8*, 139, doi:10.3389/fnins.2014.00139.

31. Buxton, R.B. Interpreting Oxygenation-Based Neuroimaging Signals: The Importance and the Challenge of Understanding Brain Oxygen Metabolism. *Front Neuroenergetics* **2010**, *2*, 8, doi:10.3389/fnene.2010.00008.

32. Buxton, R.B.; Frank, L.R. A Model for the Coupling between Cerebral Blood Flow and Oxygen Metabolism during Neural Stimulation. *J Cereb Blood Flow Metab* **1997**, *17*, 64–72, doi:10.1097/00004647-199701000-00009.

33. Van Ryckeghem, L.; Keytsman, C.; Verboven, K.; Verbaanderd, E.; Frederix, I.; Bakelants, E.; Petit, T.; Jogani, S.; Stroobants, S.; Dendale, P.; et al. Exercise Capacity Is Related to Attenuated Responses in Oxygen Extraction and Left Ventricular Longitudinal Strain in Asymptomatic Type 2 Diabetes Patients. *European Journal of Preventive Cardiology* **2021**, *28*, 1756–1766, doi:10.1093/eurjpc/zwaa007.

34. Van Ryckeghem, L.; Keytsman, C.; De Brandt, J.; Verboven, K.; Verbaanderd, E.; Marinus, N.; Franssen, W.M.A.; Frederix, I.; Bakelants, E.; Petit, T.; et al. Impact of Continuous vs. Interval Training on Oxygen Extraction and Cardiac Function during Exercise in Type 2 Diabetes Mellitus. *Eur J Appl Physiol* **2022**, *122*, 875–887, doi:10.1007/s00421-022-04884-9.

35. Kim, S.-H.; Kim, M.; Ahn, Y.-B.; Lim, H.-K.; Kang, S.-G.; Cho, J.; Park, S.-J.; Song, S.-W. Effect of Dance Exercise on Cognitive Function in Elderly Patients with Metabolic Syndrome: A Pilot Study. *J Sports Sci Med* **2011**, *10*, 671–678.

36. Holwerda, S.W.; Restaino, R.M.; Manrique, C.; Lastra, G.; Fisher, J.P.; Fadel, P.J. Augmented Pressor and Sympathetic Responses to Skeletal Muscle Metaboreflex

Activation in Type 2 Diabetes Patients. *Am J Physiol Heart Circ Physiol* **2016**, *310*, H300–H309, doi:10.1152/ajpheart.00636.2015.

37. Pinna, V.; Doneddu, A.; Roberto, S.; Magnani, S.; Ghiani, G.; Mulliri, G.; Sanna, I.; Serra, S.; Hosseini Kakhak, S.A.; Milia, R.; et al. Combined Mental Task and Metaboreflex Impair Cerebral Oxygenation in Patients with Type 2 Diabetes Mellitus. *American Journal of Physiology-Regulatory, Integrative and Comparative Physiology* **2021**, *320*, R488–R499, doi:10.1152/ajpregu.00288.2020.

38. Toth, P.; Tarantini, S.; Csiszar, A.; Ungvari, Z. Functional Vascular Contributions to Cognitive Impairment and Dementia: Mechanisms and Consequences of Cerebral Autoregulatory Dysfunction, Endothelial Impairment, and Neurovascular Uncoupling in Aging. *Am J Physiol Heart Circ Physiol* **2017**, *312*, H1–H20, doi:10.1152/ajpheart.00581.2016.

39. Bherer, L.; Erickson, K.I.; Liu-Ambrose, T. A Review of the Effects of Physical Activity and Exercise on Cognitive and Brain Functions in Older Adults. *J Aging Res* **2013**, *2013*, 657508, doi:10.1155/2013/657508.

40. Smith, J.C.; Nielson, K.A.; Antuono, P.; Lyons, J.-A.; Hanson, R.J.; Butts, A.M.; Hantke, N.C.; Verber, M.D. Semantic Memory Functional MRI and Cognitive Function after Exercise Intervention in Mild Cognitive Impairment. *Journal of Alzheimer's Disease* **2013**, *37*, 197–215, doi:10.3233/JAD-130467.

41. Liao, Y.-Y.; Chen, I.-H.; Hsu, W.-C.; Tseng, H.-Y.; Wang, R.-Y. Effect of Exergaming versus Combined Exercise on Cognitive Function and Brain Activation in Frail Older Adults: A Randomised Controlled Trial. *Ann Phys Rehabil Med* **2021**, *64*, 101492, doi:10.1016/j.rehab.2021.101492.

42. How Accurate Is the Mini-Cog Test When Used to Assess Dementia in General Practice? Available online: https://www.cochrane.org/CD011415/DEMENTIA_how-accurate-mini-cog-test-when-used-assess-dementia-general-practice (accessed on 30 May 2023).

43. Pinti, P.; Tachtsidis, I.; Hamilton, A.; Hirsch, J.; Aichelburg, C.; Gilbert, S.; Burgess, P.W. The Present and Future Use of Functional Near-infrared Spectroscopy (FNIRS) for Cognitive Neuroscience. *Annals of the New York Academy of Sciences* **2020**, *1464*, 5–29.

44. Belardinelli, R.; Georgiou, D.; Scocco, V.; Barstow, T.J.; Purcaro, A. Low Intensity Exercise Training in Patients with Chronic Heart Failure. *J Am Coll Cardiol* **1995**, *26*, 975–982, doi:10.1016/0735-1097(95)00267-1.

45. Grassi, B.; Quaresima, V.; Marconi, C.; Ferrari, M.; Cerretelli, P. Blood Lactate Accumulation and Muscle Deoxygenation during Incremental Exercise. *J Appl Physiol (1985)* **1999**, *87*, 348–355, doi:10.1152/jappl.1999.87.1.348.

46. van der Zwaard, S.; de Ruiter, C.J.; Noordhof, D.A.; Sterrenburg, R.; Bloemers, F.W.; de Koning, J.J.; Jaspers, R.T.; van der Laarse, W.J. Maximal Oxygen Uptake Is Proportional to Muscle Fiber Oxidative Capacity, from Chronic Heart Failure Patients

to Professional Cyclists. *Journal of Applied Physiology* **2016**, *121*, 636–645, doi:10.1152/japplphysiol.00355.2016.

47. Egan, B.; Zierath, J.R. Exercise Metabolism and the Molecular Regulation of Skeletal Muscle Adaptation. *Cell Metabolism* **2013**, *17*, 162–184, doi:10.1016/j.cmet.2012.12.012.
48. Barstow, T.J. Understanding near Infrared Spectroscopy and Its Application to Skeletal Muscle Research. *J Appl Physiol (1985)* **2019**, *126*, 1360–1376, doi:10.1152/japplphysiol.00166.2018.
49. Farzam, P.; Starkweather, Z.; Franceschini, M.A. Validation of a Novel Wearable, Wireless Technology to Estimate Oxygen Levels and Lactate Threshold Power in the Exercising Muscle. *Physiological Reports* **2018**, *6*, e13664, doi:10.14814/phy2.13664.
50. Jones, S.; Chiesa, S.T.; Chaturvedi, N.; Hughes, A.D. Recent Developments in Near-Infrared Spectroscopy (NIRS) for the Assessment of Local Skeletal Muscle Microvascular Function and Capacity to Utilise Oxygen. *Artery Research* **2016**, *16*, 25–33, doi:10.1016/j.artres.2016.09.001.
51. Lagerwaard, B.; Nieuwenhuizen, A.G.; de Boer, V.C.J.; Keijer, J. In Vivo Assessment of Mitochondrial Capacity Using NIRS in Locomotor Muscles of Young and Elderly Males with Similar Physical Activity Levels. *GeroScience* **2019**, *42*, 299–310, doi:10.1007/s11357-019-00145-4.
52. Boone, J.; Celie, B.; Dumortier, J.; Barstow, T.J.; De Bleecker, J.; Smet, J.; Van Lander, A.; Van Coster, R.; Bourgois, J. Forearm Muscle Oxygenation Responses during and Following Arterial Occlusion in Patients with Mitochondrial Myopathy. *Respiratory Physiology & Neurobiology* **2014**, *190*, 70–75, doi:10.1016/j.resp.2013.09.007.
53. Malagoni, A.M.; Felisatti, M.; Mandini, S.; Mascoli, F.; Manfredini, R.; Basaglia, N.; Zamboni, P.; Manfredini, F. Resting Muscle Oxygen Consumption by Near-Infrared Spectroscopy in Peripheral Arterial Disease: A Parameter to Be Considered in a Clinical Setting? *Angiology* **2010**, *61*, 530–536, doi:10.1177/0003319710362975.
54. Vardi, M.; Nini, A. Near-Infrared Spectroscopy for Evaluation of Peripheral Vascular Disease. A Systematic Review of Literature. *European Journal of Vascular and Endovascular Surgery* **2008**, *35*, 68–74, doi:10.1016/j.ejvs.2007.07.015.
55. Malagoni, A.M.; Felisatti, M.; Lamberti, N.; Basaglia, N.; Manfredini, R.; Salvi, F.; Zamboni, P.; Manfredini, F. Muscle Oxygen Consumption by NIRS and Mobility in Multiple Sclerosis Patients. *BMC Neurol* **2013**, *13*, 52, doi:10.1186/1471-2377-13-52.
56. Fu, T.-C.; Wang, C.-H.; Lin, P.-S.; Hsu, C.-C.; Cherng, W.-J.; Huang, S.-C.; Liu, M.-H.; Chiang, C.-L.; Wang, J.-S. Aerobic Interval Training Improves Oxygen Uptake Efficiency by Enhancing Cerebral and Muscular Hemodynamics in Patients with Heart Failure. *Int J Cardiol* **2013**, *167*, 41–50, doi:10.1016/j.ijcard.2011.11.086.

57. Southern, W.M.; Ryan, T.E.; Kepple, K.; Murrow, J.R.; Nilsson, K.R.; McCully, K.K. Reduced Skeletal Muscle Oxidative Capacity and Impaired Training Adaptations in Heart Failure. *Physiol Rep* **2015**, *3*, e12353, doi:10.14814/phy2.12353.

58. Belardinelli, R.; Barstow, T.J.; Porszasz, J.; Wasserman, K. Changes in Skeletal Muscle Oxygenation during Incremental Exercise Measured with near Infrared Spectroscopy. *Eur J Appl Physiol Occup Physiol* **1995**, *70*, 487–492, doi:10.1007/BF00634377.

59. Zwaard, S. van der; Jaspers, R.T.; Blokland, I.J.; Achterberg, C.; Visser, J.M.; Uil, A.R. den; Hofmijster, M.J.; Levels, K.; Noordhof, D.A.; Haan, A. de; et al. Oxygenation Threshold Derived from Near-Infrared Spectroscopy: Reliability and Its Relationship with the First Ventilatory Threshold. *PLOS ONE* **2016**, *11*, e0162914, doi:10.1371/journal.pone.0162914.

60. Wang, L.; Yoshikawa, T.; Hara, T.; Nakao, H.; Suzuki, T.; Fujimoto, S. Which Common NIRS Variable Reflects Muscle Estimated Lactate Threshold Most Closely? *Appl Physiol Nutr Metab* **2006**, *31*, 612–620, doi:10.1139/h06-069.

61. Zhao, F.; Cheung, M.; Dutta, A.; Fisher, N.; Tomita, M. Exercises to Determine Older Adults' Muscle Oxygenation Change Rate by Various Physical Performance Levels. *Archives of Physical Medicine and Rehabilitation* **2019**, *100*, e178–e179, doi:10.1016/j.apmr.2019.10.049.

62. Wahl, M.P.; Scalzo, R.L.; Regensteiner, J.G.; Reusch, J.E.B. Mechanisms of Aerobic Exercise Impairment in Diabetes: A Narrative Review. *Front Endocrinol (Lausanne)* **2018**, *9*, 181, doi:10.3389/fendo.2018.00181.

63. Kim, Y.-S.; Seifert, T.; Brassard, P.; Rasmussen, P.; Vaag, A.; Nielsen, H.B.; Secher, N.H.; van Lieshout, J.J. Impaired Cerebral Blood Flow and Oxygenation during Exercise in Type 2 Diabetic Patients. *Physiol Rep* **2015**, *3*, e12430, doi:10.14814/phy2.12430.

64. Fowler, M.J. Microvascular and Macrovascular Complications of Diabetes. *Clinical Diabetes* **2008**, *26*, 77–82, doi:10.2337/diaclin.26.2.77.

65. Rask-Madsen, C.; King, G.L. Vascular Complications of Diabetes: Mechanisms of Injury and Protective Factors. *Cell Metab* **2013**, *17*, 20–33, doi:10.1016/j.cmet.2012.11.012.

66. McClatchey, P.M.; Schafer, M.; Hunter, K.S.; Reusch, J.E.B. The Endothelial Glycocalyx Promotes Homogenous Blood Flow Distribution within the Microvasculature. *Am J Physiol Heart Circ Physiol* **2016**, *311*, H168–H176, doi:10.1152/ajpheart.00132.2016.

67. Dogné, S.; Flamion, B.; Caron, N. Endothelial Glycocalyx as a Shield Against Diabetic Vascular Complications. *Arterioscler Thromb Vasc Biol* **2018**, *38*, 1427–1439, doi:10.1161/ATVBAHA.118.310839.

68. Kröpfl, J.M.; Beltrami, F.G.; Rehm, M.; Gruber, H.-J.; Stelzer, I.; Spengler, C.M. Acute Exercise-Induced Glycocalyx Shedding Does Not Differ between Exercise Modalities, but Is Associated with Total Antioxidative Capacity. *Journal of Science and Medicine in Sport* **2021**, *24*, 689–695, doi:10.1016/j.jsams.2021.01.010.

69. Schmitz, B.; Niehues, H.; Lenders, M.; Thorwesten, L.; Klose, A.; Krüger, M.; Brand, E.; Brand, S.-M. Effects of High-Intensity Interval Training on Microvascular Glycocalyx and Associated MicroRNAs. *American Journal of Physiology-Heart and Circulatory Physiology* **2019**, *316*, H1538–H1551, doi:10.1152/ajpheart.00751.2018.

70. Machin, D.R.; Phuong, T.T.T.; Donato, A.J. The Role of the Endothelial Glycocalyx in Advanced Age and Cardiovascular Disease. *Curr Opin Pharmacol* **2019**, *45*, 66–71, doi:10.1016/j.coph.2019.04.011.

71. Hahn, R.G.; Patel, V.; Dull, R.O. Human Glycocalyx Shedding: Systematic Review and Critical Appraisal. *Acta Anaesthesiologica Scandinavica* **2021**, *65*, 590–606, doi:10.1111/aas.13797.

72. Targosz-Korecka, M.; Jaglarz, M.; Malek-Zietek, K.E.; Gregorius, A.; Zakrzewska, A.; Sitek, B.; Rajfur, Z.; Chlopicki, S.; Szymonski, M. AFM-Based Detection of Glycocalyx Degradation and Endothelial Stiffening in the Db/Db Mouse Model of Diabetes. *Sci Rep* **2017**, *7*, 15951, doi:10.1038/s41598-017-16179-7.

73. Sandoo, A.; van Zanten, J.J.C.S.V.; Metsios, G.S.; Carroll, D.; Kitas, G.D. The Endothelium and Its Role in Regulating Vascular Tone. *Open Cardiovasc Med J* **2010**, *4*, 302–312, doi:10.2174/1874192401004010302.

74. Harrison, D.G. Endothelial Control of Vasomotion and Nitric Oxide Production: A Potential Target for Risk Factor Management. *Cardiol Clin* **1996**, *14*, 1–15, doi:10.1016/s0733-8651(05)70257-5.

75. Haselden, W.D.; Kedarasetti, R.T.; Drew, P.J. Spatial and Temporal Patterns of Nitric Oxide Diffusion and Degradation Drive Emergent Cerebrovascular Dynamics. *PLOS Computational Biology* **2020**, *16*, e1008069, doi:10.1371/journal.pcbi.1008069.

76. Harrison, D.G.; Widder, J.; Grumbach, I.; Chen, W.; Weber, M.; Searles, C. Endothelial Mechanotransduction, Nitric Oxide and Vascular Inflammation. *Journal of Internal Medicine* **2006**, *259*, 351–363, doi:10.1111/j.1365-2796.2006.01621.x.

77. Kalra, S.; Sahay, R. Diabetes Fatigue Syndrome. *Diabetes Ther* **2018**, *9*, 1421–1429, doi:10.1007/s13300-018-0453-x.

78. Berg, J.M.; Tymoczko, J.L.; Stryer, L. *Biochemistry*; 5th ed.; W.H. Freeman ; NCBI: New York, [Bethesda, MD], 2002;

79. Kemp, G.J.; Hands, L.J.; Ramaswami, G.; Taylor, D.J.; Nicolaides, A.; Amato, A.; Radda, G.K. Calf Muscle Mitochondrial and Glycogenolytic Atp Synthesis in Patients with Claudication Due to Peripheral Vascular Disease Analysed Using 31P Magnetic Resonance Spectroscopy. *Clinical Science* **1995**, *89*, 581–590, doi:10.1042/cs0890581.

80. Bauer, T.A.; Reusch, J.E.B.; Levi, M.; Regensteiner, J.G. Skeletal Muscle Deoxygenation After the Onset of Moderate Exercise Suggests Slowed Microvascular Blood Flow Kinetics in Type 2 Diabetes. *Diabetes Care* **2007**, *30*, 2880–2885, doi:10.2337/dc07-0843.

81. Zhao, F.; Tomita, M.R.; Dutta, A. Functional Near-Infrared Spectroscopy of Prefrontal Cortex during Memory Encoding and Recall in Elderly with Type 2 Diabetes Mellitus. *Annu Int Conf IEEE Eng Med Biol Soc* **2022**, *2022*, 3323–3326, doi:10.1109/EMBC48229.2022.9871983.

82. Das, A.; Murphy, K.; Drew, P.J. Rude Mechanicals in Brain Haemodynamics: Non-Neural Actors That Influence Blood Flow. *Philosophical Transactions of the Royal Society B: Biological Sciences* **2020**, *376*, 20190635, doi:10.1098/rstb.2019.0635.

83. Aalkjær, C.; Nilsson, H. Vasomotion: Cellular Background for the Oscillator and for the Synchronization of Smooth Muscle Cells. *Br J Pharmacol* **2005**, *144*, 605–616, doi:10.1038/sj.bjp.0706084.

84. Paniagua, O.A.; Bryant, M.B.; Panza, J.A. Role of Endothelial Nitric Oxide in Shear Stress–Induced Vasodilation of Human Microvasculature. *Circulation* **2001**, *103*, 1752–1758, doi:10.1161/01.CIR.103.13.1752.

85. Jiang, X.Z.; Goligorsky, M.S. Biomechanical Properties of Endothelial Glycocalyx: An Imperfect Pendulum. *Matrix Biol Plus* **2021**, *12*, 100087, doi:10.1016/j.mbplus.2021.100087.

86. Farina, A.; Rosso, F.; Fasano, A. A Continuum Mechanics Model for the Fåhræus-Lindqvist Effect. *J Biol Phys* **2021**, *47*, 253–270, doi:10.1007/s10867-021-09575-8.

87. Forouzan, O.; Yang, X.; Sosa, J.M.; Burns, J.M.; Shevkoplyas, S.S. Spontaneous Oscillations of Capillary Blood Flow in Artificial Microvascular Networks. *Microvasc Res* **2012**, *84*, 123–132, doi:10.1016/j.mvr.2012.06.006.

88. Au, S.-K.; Brownjohn, J.M.W.; Li, B.; Raby, A. Understanding and Managing Identification Uncertainty of Close Modes in Operational Modal Analysis. *Mechanical Systems and Signal Processing* **2021**, *147*, 107018, doi:10.1016/j.ymssp.2020.107018.

89. Akazawa, N.; Tanahashi, K.; Kosaki, K.; Ra, S.; Matsubara, T.; Choi, Y.; Zempo-Miyaki, A.; Maeda, S. Aerobic Exercise Training Enhances Cerebrovascular Pulsatility Response to Acute Aerobic Exercise in Older Adults. *Physiol Rep* **2018**, *6*, e13681, doi:10.14814/phy2.13681.

90. Zhang, Y.; Zeng, J.; He, X.; Cao, W.; Peng, X.; Li, G. Pulsatility Protects the Endothelial Glycocalyx during Extracorporeal Membrane Oxygenation. *Microcirculation* **2021**, *28*, e12722, doi:10.1111/micc.12722.

91. Meyer, M.L.; Palta, P.; Tanaka, H.; Deal, J.A.; Wright, J.; Knopman, D.S.; Griswold, M.E.; Mosley, T.H.; Heiss, G. Association of Central Arterial Stiffness and Pressure Pulsatility with Mild Cognitive Impairment and Dementia: The Atherosclerosis Risk

in Communities Study-Neurocognitive Study (ARIC-NCS). *J. Alzheimers Dis.* **2017**, *57*, 195–204, doi:10.3233/JAD-161041.

92. Nieuwdorp, M.; van Haeften, T.W.; Gouverneur, M.C.L.G.; Mooij, H.L.; van Lieshout, M.H.P.; Levi, M.; Meijers, J.C.M.; Holleman, F.; Hoekstra, J.B.L.; Vink, H.; et al. Loss of Endothelial Glycocalyx During Acute Hyperglycemia Coincides With Endothelial Dysfunction and Coagulation Activation In Vivo. *Diabetes* **2006**, *55*, 480–486, doi:10.2337/diabetes.55.02.06.db05-1103.

93. Jahani, S.; Fantana, A.L.; Harper, D.; Ellison, J.M.; Boas, D.A.; Forester, B.P.; Yücel, M.A. FNIRS Can Robustly Measure Brain Activity during Memory Encoding and Retrieval in Healthy Subjects. *Scientific Reports* **2017**, *7*, 9533, doi:10.1038/s41598-017-09868-w.

94. Sun, S.; Yang, B.; Zhang, Q.; Wüchner, R.; Pan, L.; Zhu, H. Fast Online Implementation of Covariance-Driven Stochastic Subspace Identification. *Mechanical Systems and Signal Processing* **2023**, *197*, 110326, doi:10.1016/j.ymssp.2023.110326.

95. Zhao, F. Cerebral and Muscular Oxygenation Changes after Moderate-Intensity Exercise in Sedentary Older Adults with Type 2 Diabetes. Ph.D., State University of New York at Buffalo: United States -- New York, 2022.

96. Colberg, S.R.; Sigal, R.J.; Fernhall, B.; Regensteiner, J.G.; Blissmer, B.J.; Rubin, R.R.; Chasan-Taber, L.; Albright, A.L.; Braun, B.; American College of Sports Medicine; et al. Exercise and Type 2 Diabetes: The American College of Sports Medicine and the American Diabetes Association: Joint Position Statement. *Diabetes Care* **2010**, *33*, e147-167, doi:10.2337/dc10-9990.

97. Irvine, C.; Taylor, N.F. Progressive Resistance Exercise Improves Glycaemic Control in People with Type 2 Diabetes Mellitus: A Systematic Review. *Aust J Physiother* **2009**, *55*, 237–246, doi:10.1016/s0004-9514(09)70003-0.

98. Bennett, J.A.; Winters-Stone, K.; Nail, L.M.; Scherer, J. Definitions of Sedentary in Physical-Activity-Intervention Trials: A Summary of the Literature. *J Aging Phys Act* **2006**, *14*, 456–477, doi:10.1123/japa.14.4.456.

99. Murkin, J.M.; Arango, M. Near-Infrared Spectroscopy as an Index of Brain and Tissue Oxygenation. *British Journal of Anaesthesia* **2009**, *103*, i3–i13, doi:10.1093/bja/aep299.

100. Huppert, T.J.; Hoge, R.D.; Diamond, S.G.; Franceschini, M.A.; Boas, D.A. A Temporal Comparison of BOLD, ASL, and NIRS Hemodynamic Responses to Motor Stimuli in Adult Humans. *Neuroimage* **2006**, *29*, 368–382, doi:10.1016/j.neuroimage.2005.08.065.

101. Mehagnoul-Schipper, D.J.; van der Kallen, B.F.W.; Colier, W.N.J.M.; van der Sluijs, M.C.; van Erning, L.J.T.O.; Thijssen, H.O.M.; Oeseburg, B.; Hoefnagels, W.H.L.; Jansen, R.W.M.M. Simultaneous Measurements of Cerebral Oxygenation Changes during Brain Activation by Near-Infrared Spectroscopy and Functional

Magnetic Resonance Imaging in Healthy Young and Elderly Subjects. *Hum Brain Mapp* **2002**, *16*, 14–23, doi:10.1002/hbm.10026.

102. Huppert, T.J.; Diamond, S.G.; Franceschini, M.A.; Boas, D.A. HomER: A Review of Time-Series Analysis Methods for near-Infrared Spectroscopy of the Brain. *Appl Opt* **2009**, *48*, D280–D298.

103. Arora, Y.; Dutta, A. Perspective: Disentangling the Effects of TES on Neurovascular Unit. *Frontiers in Neurology* **2023**, *13*.

104. Santosa, H.; Zhai, X.; Fishburn, F.; Huppert, T. The NIRS Brain AnalyzIR Toolbox. *Algorithms* **2018**, *11*, 73, doi:10.3390/a11050073.

105. Barker, J.W.; Aarabi, A.; Huppert, T.J. Autoregressive Model Based Algorithm for Correcting Motion and Serially Correlated Errors in FNIRS. *Biomed Opt Express* **2013**, *4*, 1366–1379, doi:10.1364/BOE.4.001366.

106. Brincker, R.; Andersen, P.; Jacobsen, N.-J. Automated Frequency Domain Decomposition for Operational Modal Analysis.; 2007.

107. Brincker, R.; Zhang, L.; Andersen, P. Modal Identification of Output-Only Systems Using Frequency Domain Decomposition. *Smart Mater. Struct.* **2001**, *10*, 441, doi:10.1088/0964-1726/10/3/303.

108. Arora, Y.; Dutta, A. Human-In-The-Loop Optimization of Transcranial Electrical Stimulation Effects: A Computational Perspective Based on Systems Analysis 2022.

109. Arora, Y.; Walia, P.; Hayashibe, M.; Muthalib, M.; Chowdhury, S.R.; Perrey, S.; Dutta, A. Grey-Box Modeling and Hypothesis Testing of Functional near-Infrared Spectroscopy-Based Cerebrovascular Reactivity to Anodal High-Definition TDCS in Healthy Humans. *PLOS Computational Biology* **2021**, *17*, e1009386, doi:10.1371/journal.pcbi.1009386.

110. Bicciato, G.; Keller, E.; Wolf, M.; Brandi, G.; Schulthess, S.; Friedl, S.G.; Willms, J.F.; Narula, G. Increase in Low-Frequency Oscillations in FNIRS as Cerebral Response to Auditory Stimulation with Familiar Music. *Brain Sci* **2021**, *12*, 42, doi:10.3390/brainsci12010042.

111. Neu, E.; Janser, F.; Khatibi, A.A.; Orifici, A.C. Fully Automated Operational Modal Analysis Using Multi-Stage Clustering. *Mechanical Systems and Signal Processing* **2017**, *84*, 308–323, doi:10.1016/j.ymssp.2016.07.031.

112. Crum, E.M.; O'Connor, W.J.; Van Loo, L.; Valckx, M.; Stannard, S.R. Validity and Reliability of the Moxy Oxygen Monitor during Incremental Cycling Exercise. *Eur J Sport Sci* **2017**, *17*, 1037–1043, doi:10.1080/17461391.2017.1330899.

113. Borson, S.; Scanlan, J.; Brush, M.; Vitaliano, P.; Dokmak, A. The Mini-Cog: A Cognitive "vital Signs" Measure for Dementia Screening in Multi-Lingual Elderly. *Int J Geriatr Psychiatry* **2000**, *15*, 1021–1027, doi:10.1002/1099-1166(200011)15:11<1021::aid-gps234>3.0.co;2-6.

114. Tsoi, K.K.F.; Chan, J.Y.C.; Hirai, H.W.; Wong, S.Y.S.; Kwok, T.C.Y. Cognitive Tests to Detect Dementia: A Systematic Review and Meta-Analysis. *JAMA Intern Med* **2015**, *175*, 1450–1458, doi:10.1001/jamainternmed.2015.2152.

115. Balke, B. A SIMPLE FIELD TEST FOR THE ASSESSMENT OF PHYSICAL FITNESS. REP 63-6. *Rep Civ Aeromed Res Inst US* **1963**, 1–8.

116. Chan, W.L.; Chan, H.L.; Chen, K.M.; Fan, H.L.; Lai, W.C.; Yu, S.W. Reliability and Validity of Walk Tests for Older Adults with Dementia: A Systematic Review. *Alzheimer's & Dementia* **2021**, *17*, e050371, doi:10.1002/alz.050371.

117. Lunsford, B.R.; Perry, J. The Standing Heel-Rise Test for Ankle Plantar Flexion: Criterion for Normal. *Physical Therapy* **1995**, *75*, 694–698, doi:10.1093/ptj/75.8.694.

118. Fairclough, S.H.; Burns, C.; Kreplin, U. FNIRS Activity in the Prefrontal Cortex and Motivational Intensity: Impact of Working Memory Load, Financial Reward, and Correlation-Based Signal Improvement. *Neurophotonics* **2018**, *5*, 035001, doi:10.1117/1.NPh.5.3.035001.

119. du Boisgueheneuc, F.; Levy, R.; Volle, E.; Seassau, M.; Duffau, H.; Kinkingnehun, S.; Samson, Y.; Zhang, S.; Dubois, B. Functions of the Left Superior Frontal Gyrus in Humans: A Lesion Study. *Brain* **2006**, *129*, 3315–3328, doi:10.1093/brain/awl244.

120. Rolls, E.T.; Huang, C.-C.; Lin, C.-P.; Feng, J.; Joliot, M. Automated Anatomical Labelling Atlas 3. *NeuroImage* **2020**, *206*, 116189, doi:10.1016/j.neuroimage.2019.116189.

121. Hu, S.; Ide, J.S.; Zhang, S.; Li, C.R. The Right Superior Frontal Gyrus and Individual Variation in Proactive Control of Impulsive Response. *J. Neurosci.* **2016**, *36*, 12688–12696, doi:10.1523/JNEUROSCI.1175-16.2016.

122. Cerebral Correlates of Autonomic Cardiovascular Arousal: A Functional Neuroimaging Investigation in Humans.

123. ter Laan, M.; van Dijk, J.M.C.; Elting, J.W.J.; Staal, M.J.; Absalom, A.R. Sympathetic Regulation of Cerebral Blood Flow in Humans: A Review. *British Journal of Anaesthesia* **2013**, *111*, 361–367, doi:10.1093/bja/aet122.

124. Stanford, K.I.; Goodyear, L.J. Muscle-Adipose Tissue Cross Talk. *Cold Spring Harb Perspect Med* **2018**, *8*, a029801, doi:10.1101/cshperspect.a029801.

125. Rosano, C.; Newman, A.; Santanasto, A.; Zhu, X.; Goodpaster, B.; Miljkovic, I. Increase in Skeletal Muscular Adiposity and Cognitive Decline in a Biracial Cohort of Older Men and Women. *J Am Geriatr Soc* **2023**, doi:10.1111/jgs.18419.

126. Silveira-Rodrigues, J.G.; Pires, W.; Gomes, P.F.; Ogando, P.H.M.; Melo, B.P.; Aleixo, I.M.S.; Soares, D.D. Combined Exercise Training Improves Specific Domains of Cognitive Functions and Metabolic Markers in Middle-Aged and Older Adults with Type 2 Diabetes Mellitus. *Diabetes Res Clin Pract* **2021**, *173*, 108700, doi:10.1016/j.diabres.2021.108700.

127. Leischik, R.; Schwarz, K.; Bank, P.; Brzek, A.; Dworrak, B.; Strauss, M.; Litwitz, H.; Gerlach, C.E. Exercise Improves Cognitive Function-A Randomized Trial on the Effects of Physical Activity on Cognition in Type 2 Diabetes Patients. *J Pers Med* **2021**, *11*, 530, doi:10.3390/jpm11060530.

128. Berchicci, M.; Lucci, G.; Di Russo, F. Benefits of Physical Exercise on the Aging Brain: The Role of the Prefrontal Cortex. *J Gerontol A Biol Sci Med Sci* **2013**, *68*, 1337–1341, doi:10.1093/gerona/glt094.

129. Liao, Y.-Y.; Chen, I.-H.; Wang, R.-Y. Effects of Kinect-Based Exergaming on Frailty Status and Physical Performance in Prefrail and Frail Elderly: A Randomized Controlled Trial. *Sci Rep* **2019**, *9*, 9353, doi:10.1038/s41598-019-45767-y.

130. Bertram, S.; Brixius, K.; Brinkmann, C. Exercise for the Diabetic Brain: How Physical Training May Help Prevent Dementia and Alzheimer's Disease in T2DM Patients. *Endocrine* **2016**, *53*, 350–363, doi:10.1007/s12020-016-0976-8.

131. Lustig, C.; Shah, P.; Seidler, R.; Reuter-Lorenz, P.A. Aging, Training, and the Brain: A Review and Future Directions. *Neuropsychol Rev* **2009**, *19*, 504–522, doi:10.1007/s11065-009-9119-9.

132. Dickerson, B.C.; Salat, D.H.; Greve, D.N.; Chua, E.F.; Rand-Giovannetti, E.; Rentz, D.M.; Bertram, L.; Mullin, K.; Tanzi, R.E.; Blacker, D.; et al. Increased Hippocampal Activation in Mild Cognitive Impairment Compared to Normal Aging and AD. *Neurology* **2005**, *65*, 404–411, doi:10.1212/01.wnl.0000171450.97464.49.

133. Reuter-Lorenz, P.A.; Lustig, C. Brain Aging: Reorganizing Discoveries about the Aging Mind. *Curr Opin Neurobiol* **2005**, *15*, 245–251, doi:10.1016/j.conb.2005.03.016.

134. Bruckmaier, M.; Tachtsidis, I.; Phan, P.; Lavie, N. Attention and Capacity Limits in Perception: A Cellular Metabolism Account. *J Neurosci* **2020**, *40*, 6801–6811, doi:10.1523/JNEUROSCI.2368-19.2020.

135. Mootha, V.K.; Lindgren, C.M.; Eriksson, K.-F.; Subramanian, A.; Sihag, S.; Lehar, J.; Puigserver, P.; Carlsson, E.; Ridderstråle, M.; Laurila, E.; et al. PGC-1α-Responsive Genes Involved in Oxidative Phosphorylation Are Coordinately Downregulated in Human Diabetes. *Nat Genet* **2003**, *34*, 267–273, doi:10.1038/ng1180.

136. Patti, M.E.; Butte, A.J.; Crunkhorn, S.; Cusi, K.; Berria, R.; Kashyap, S.; Miyazaki, Y.; Kohane, I.; Costello, M.; Saccone, R.; et al. Coordinated Reduction of Genes of Oxidative Metabolism in Humans with Insulin Resistance and Diabetes: Potential Role of PGC1 and NRF1. *Proc Natl Acad Sci U S A* **2003**, *100*, 8466–8471, doi:10.1073/pnas.1032913100.

137. Petersen, K.F.; Befroy, D.; Dufour, S.; Dziura, J.; Ariyan, C.; Rothman, D.L.; DiPietro, L.; Cline, G.W.; Shulman, G.I. Mitochondrial Dysfunction in the Elderly: Possible Role in Insulin Resistance. *Science* **2003**, *300*, 1140–1142, doi:10.1126/science.1082889.

138. Schrauwen-Hinderling, V.B.; Kooi, M.E.; Hesselink, M.K.C.; Jeneson, J. a. L.; Backes, W.H.; van Echteld, C.J.A.; van Engelshoven, J.M.A.; Mensink, M.; Schrauwen, P. Impaired in Vivo Mitochondrial Function but Similar Intramyocellular Lipid Content in Patients with Type 2 Diabetes Mellitus and BMI-Matched Control Subjects. *Diabetologia* **2007**, *50*, 113–120, doi:10.1007/s00125-006-0475-1.

139. Szendroedi, J.; Schmid, A.I.; Chmelik, M.; Toth, C.; Brehm, A.; Krssak, M.; Nowotny, P.; Wolzt, M.; Waldhausl, W.; Roden, M. Muscle Mitochondrial ATP Synthesis and Glucose Transport/Phosphorylation in Type 2 Diabetes. *PLoS Med* **2007**, *4*, e154, doi:10.1371/journal.pmed.0040154.

140. Zilberter, Y.; Zilberter, M. The Vicious Circle of Hypometabolism in Neurodegenerative Diseases: Ways and Mechanisms of Metabolic Correction. *Journal of Neuroscience Research* **2017**, *95*, 2217–2235, doi:10.1002/jnr.24064.

141. Mullins, R.; Reiter, D.; Kapogiannis, D. Magnetic Resonance Spectroscopy Reveals Abnormalities of Glucose Metabolism in the Alzheimer's Brain. *Ann Clin Transl Neurol* **2018**, *5*, 262–272, doi:10.1002/acn3.530.

142. Attwell, D.; Gibb, A. Neuroenergetics and the Kinetic Design of Excitatory Synapses. *Nat Rev Neurosci* **2005**, *6*, 841–849, doi:10.1038/nrn1784.

143. Barbiellini Amidei, C.; Fayosse, A.; Dumurgier, J.; Machado-Fragua, M.D.; Tabak, A.G.; van Sloten, T.; Kivimäki, M.; Dugravot, A.; Sabia, S.; Singh-Manoux, A. Association Between Age at Diabetes Onset and Subsequent Risk of Dementia. *JAMA* **2021**, *325*, 1640–1649, doi:10.1001/jama.2021.4001.

144. Kandimalla, R.; Thirumala, V.; Reddy, P.H. Is Alzheimer's Disease a Type 3 Diabetes? A Critical Appraisal. *Biochimica et Biophysica Acta (BBA) - Molecular Basis of Disease* **2017**, *1863*, 1078–1089, doi:10.1016/j.bbadis.2016.08.018.

145. Kim, J.; Wei, Y.; Sowers, J.R. Role of Mitochondrial Dysfunction in Insulin Resistance. *Circulation Research* **2008**, *102*, 401–414, doi:10.1161/CIRCRESAHA.107.165472.

146. M.d, L.H.; Mann, J.J. Test–Retest Reliability of Brain Mitochondrial Cytochrome-c-Oxidase Assessed by Functional near-Infrared Spectroscopy. *JBO* **2018**, *23*, 056006, doi:10.1117/1.JBO.23.5.056006.

147. Dutta, A. Bidirectional Interactions between Neuronal and Hemodynamic Responses to Transcranial Direct Current Stimulation (TDCS): Challenges for Brain-State Dependent TDCS. *Frontiers in Systems Neuroscience* **2015**, 107, doi:10.3389/fnsys.2015.00107.

148. Shaw, K.; Bell, L.; Boyd, K.; Grijseels, D.M.; Clarke, D.; Bonnar, O.; Crombag, H.S.; Hall, C.N. Neurovascular Coupling and Oxygenation Are Decreased in Hippocampus Compared to Neocortex Because of Microvascular Differences. *Nat Commun* **2021**, *12*, 3190, doi:10.1038/s41467-021-23508-y.

149. Arora, Y.; Chowdhury, S.R.; Dutta, A. Physiological Neurovascular Modeling of Cerebrovascular Effects of Transcranial Electrical Current Stimulation. *Brain Stimulation: Basic, Translational, and Clinical Research in Neuromodulation* **2021**, *14*, 1597–1598, doi:10.1016/j.brs.2021.10.031.

150. Fujii, H.; Ito, H.; Aihara, K.; Ichinose, N.; Tsukada, M. Dynamical Cell Assembly Hypothesis — Theoretical Possibility of Spatio-Temporal Coding in the Cortex. *Neural Networks* **1996**, *9*, 1303–1350, doi:10.1016/S0893-6080(96)00054-8.

151. Stefanovska, A.; Bracic, M.; Kvernmo, H.D. Wavelet Analysis of Oscillations in the Peripheral Blood Circulation Measured by Laser Doppler Technique. *IEEE Trans Biomed Eng* **1999**, *46*, 1230–1239, doi:10.1109/10.790500.

152. Gibbons, C.H.; Freeman, R. Treatment-Induced Neuropathy of Diabetes: An Acute, Iatrogenic Complication of Diabetes. *Brain* **2015**, *138*, 43–52, doi:10.1093/brain/awu307.

153. Geddes, J.B.; Carr, R.T.; Wu, F.; Lao, Y.; Maher, M. Blood Flow in Microvascular Networks: A Study in Nonlinear Biology. *Chaos* **2010**, *20*, 045123, doi:10.1063/1.3530122.

154. Irace, C.; Carallo, C.; Scavelli, F.; De Franceschi, M.S.; Esposito, T.; Gnasso, A. Blood Viscosity in Subjects with Normoglycemia and Prediabetes. *Diabetes Care* **2014**, *37*, 488–492, doi:10.2337/dc13-1374.

155. Kistenmacher, A.; Manneck, S.; Wardzinski, E.K.; Martens, J.C.; Gohla, G.; Melchert, U.H.; Jauch-Chara, K.; Oltmanns, K.M. Persistent Blood Glucose Reduction upon Repeated Transcranial Electric Stimulation in Men. *Brain Stimul* **2017**, *10*, 780–786, doi:10.1016/j.brs.2017.03.011.

156. Scholey, A.B.; Harper, S.; Kennedy, D.O. Cognitive Demand and Blood Glucose. *Physiol Behav* **2001**, *73*, 585–592, doi:10.1016/s0031-9384(01)00476-0.

157. Chan, C.C.; Fage, B.A.; Burton, J.K.; Smailagic, N.; Gill, S.S.; Herrmann, N.; Nikolaou, V.; Quinn, T.J.; Noel-Storr, A.H.; Seitz, D.P. Mini-Cog for the Diagnosis of Alzheimer's Disease Dementia and Other Dementias within a Secondary Care Setting. *Cochrane Database Syst Rev* **2019**, *9*, CD011414, doi:10.1002/14651858.CD011414.pub2.

158. Zhao, F.; Tomita, M.; Dutta, A. Functional Near-Infrared Spectroscopy Of Prefrontal Cortex During Memory Encoding And Recall In Elderly With Type 2 Diabetes Mellitus. **2022**, doi:10.20944/preprints202202.0045.v1.

159. Wong, A.D.; Ye, M.; Levy, A.F.; Rothstein, J.D.; Bergles, D.E.; Searson, P.C. The Blood-Brain Barrier: An Engineering Perspective. *Front Neuroeng* **2013**, *6*, 7, doi:10.3389/fneng.2013.00007.

160. Arnold, S.E.; Arvanitakis, Z.; Macauley-Rambach, S.L.; Koenig, A.M.; Wang, H.-Y.; Ahima, R.S.; Craft, S.; Gandy, S.; Buettner, C.; Stoeckel, L.E.; et al. Brain Insulin

Resistance in Type 2 Diabetes and Alzheimer Disease: Concepts and Conundrums. *Nat Rev Neurol* **2018**, *14*, 168–181, doi:10.1038/nrneurol.2017.185.

161. Demarest, T.G.; Varma, V.R.; Estrada, D.; Babbar, M.; Basu, S.; Mahajan, U.V.; Moaddel, R.; Croteau, D.L.; Thambisetty, M.; Mattson, M.P.; et al. Biological Sex and DNA Repair Deficiency Drive Alzheimer's Disease via Systemic Metabolic Remodeling and Brain Mitochondrial Dysfunction. *Acta Neuropathol* **2020**, *140*, 25–47, doi:10.1007/s00401-020-02152-8.

162. Karanth, S.S.; Mujumdar, R.; Sahoo, J.P.; Das, A.; Stachowiak, M.K.; Dutta, A. Human Brain Organoid Platform for Neuroengineering Optical Theranostics in Neonatal Sepsis. In Proceedings of the Converging Clinical and Engineering Research on Neurorehabilitation IV; Torricelli, D., Akay, M., Pons, J.L., Eds.; Springer International Publishing: Cham, 2022; pp. 753–757.

163. Lombardi, F.; Herrmann, H.J.; de Arcangelis, L. Balance of Excitation and Inhibition Determines 1/f Power Spectrum in Neuronal Networks. *Chaos* **2017**, *27*, 047402, doi:10.1063/1.4979043.

164. Dutta, A.; Karanth, S.S.; Bhattacharya, M.; Liput, M.; Augustyniak, J.; Cheung, M.; Stachowiak, E.K.; Stachowiak, M.K. A Proof of Concept 'Phase Zero' Study of Neurodevelopment Using Brain Organoid Models with Vis/near-Infrared Spectroscopy and Electrophysiology. *Scientific Reports* **2020**, *10*, 20987, doi:10.1038/s41598-020-77929-8.

165. Zhang, L.; Su, F.; Buizer, S.; Lu, H.; Gao, W.; Tian, Y.; Meldrum, D. A Dual Sensor for Real-Time Monitoring of Glucose and Oxygen. *Biomaterials* **2013**, *34*, 10.1016/j.biomaterials.2013.09.031, doi:10.1016/j.biomaterials.2013.09.031.

166. Arora, Y.; Dutta, A. Human-in-the-Loop Optimization of Transcranial Electrical Stimulation at the Point of Care: A Computational Perspective. *Brain Sciences* **2022**, *12*, 1294, doi:10.3390/brainsci12101294.

167. Zhao, X.; Xu, Z.; Xiao, L.; Shi, T.; Xiao, H.; Wang, Y.; Li, Y.; Xue, F.; Zeng, W. Review on the Vascularization of Organoids and Organoids-on-a-Chip. *Frontiers in Bioengineering and Biotechnology* **2021**, *9*.

168. Arora, Y.; Walia, P.; Hayashibe, M.; Muthalib, M.; Chowdhury, S.R.; Perrey, S.; Dutta, A. Grey-Box Modeling and Hypothesis Testing of Functional near-Infrared Spectroscopy-Based Cerebrovascular Reactivity to Anodal High-Definition TDCS in Healthy Humans 2021.

169. Petrou, M.; Pop-Busui, R.; Foerster, B.R.; Edden, R.A.; Callaghan, B.C.; Harte, S.E.; Harris, R.E.; Clauw, D.J.; Feldman, E.L. Altered Excitation-Inhibition Balance in the Brain of Patients with Diabetic Neuropathy. *Acad Radiol* **2012**, *19*, 607–612, doi:10.1016/j.acra.2012.02.004.

170. Sood, M.; Besson, P.; Muthalib, M.; Jindal, U.; Perrey, S.; Dutta, A.; Hayashibe, M. NIRS-EEG Joint Imaging during Transcranial Direct Current Stimulation: Online

Parameter Estimation with an Autoregressive Model. *J. Neurosci. Methods* **2016**, *274*, 71–80, doi:10.1016/j.jneumeth.2016.09.008.

171. Nitsche, M.A.; Paulus, W. Excitability Changes Induced in the Human Motor Cortex by Weak Transcranial Direct Current Stimulation. *J. Physiol. (Lond.)* **2000**, *527 Pt 3*, 633–639.

172. Jamil, A.; Batsikadze, G.; Kuo, H.-I.; Meesen, R.L.J.; Dechent, P.; Paulus, W.; Nitsche, M.A. Current Intensity- and Polarity-Specific Online and Aftereffects of Transcranial Direct Current Stimulation: An FMRI Study. *Human Brain Mapping* **2020**, *41*, 1644–1666, doi:10.1002/hbm.24901.

173. Bahr-Hosseini, M.; Bikson, M. Neurovascular-Modulation: A Review of Primary Vascular Responses to Transcranial Electrical Stimulation as a Mechanism of Action. *Brain Stimulation* **2021**, *14*, 837–847, doi:10.1016/j.brs.2021.04.015.

174. Dutta, A.; Jacob, A.; Chowdhury, S.R.; Das, A.; Nitsche, M.A. EEG-NIRS Based Assessment of Neurovascular Coupling during Anodal Transcranial Direct Current Stimulation--a Stroke Case Series. *J Med Syst* **2015**, *39*, 205, doi:10.1007/s10916-015-0205-7.

175. Dutta, A. Simultaneous Functional Near-Infrared Spectroscopy (FNIRS) and Electroencephalogram (EEG) to Elucidate Neurovascular Modulation by Transcranial Electrical Stimulation (TES). *Brain Stimul* **2021**, *14*, 1093–1094, doi:10.1016/j.brs.2021.07.019.

176. Grubb, S.; Cai, C.; Hald, B.O.; Khennouf, L.; Murmu, R.P.; Jensen, A.G.K.; Fordsmann, J.; Zambach, S.; Lauritzen, M. Precapillary Sphincters Maintain Perfusion in the Cerebral Cortex. *Nat Commun* **2020**, *11*, 395, doi:10.1038/s41467-020-14330-z.

177. Zambach, S.A.; Cai, C.; Helms, H.C.C.; Hald, B.O.; Dong, Y.; Fordsmann, J.C.; Nielsen, R.M.; Hu, J.; Lønstrup, M.; Brodin, B.; et al. Precapillary Sphincters and Pericytes at First-Order Capillaries as Key Regulators for Brain Capillary Perfusion. *Proc Natl Acad Sci U S A* **2021**, *118*, e2023749118, doi:10.1073/pnas.2023749118.

178. Lundgaard, I.; Li, B.; Xie, L.; Kang, H.; Sanggaard, S.; Haswell, J.D.R.; Sun, W.; Goldman, S.; Blekot, S.; Nielsen, M.; et al. Direct Neuronal Glucose Uptake Heralds Activity-Dependent Increases in Cerebral Metabolism. *Nat Commun* **2015**, *6*, 6807, doi:10.1038/ncomms7807.

179. Drew, P.J.; Mateo, C.; Turner, K.L.; Yu, X.; Kleinfeld, D. Ultra-Slow Oscillations in FMRI and Resting-State Connectivity: Neuronal and Vascular Contributions and Technical Confounds. *Neuron* **2020**, *107*, 782–804, doi:10.1016/j.neuron.2020.07.020.

180. van Veluw, S.J.; Hou, S.S.; Calvo-Rodriguez, M.; Arbel-Ornath, M.; Snyder, A.C.; Frosch, M.P.; Greenberg, S.M.; Bacskai, B.J. Vasomotion as a Driving Force for Paravascular Clearance in the Awake Mouse Brain. *Neuron* **2020**, *105*, 549-561.e5, doi:10.1016/j.neuron.2019.10.033.

181. Dagar, S.; Chowdhury, S.R.; Bapi, R.S.; Dutta, A.; Roy, D. Near-Infrared Spectroscopy – Electroencephalography-Based Brain-State-Dependent Electrotherapy: A Computational Approach Based on Excitation–Inhibition Balance Hypothesis. *Front Neurol* **2016**, *7*, doi:10.3389/fneur.2016.00123.

182. A ‘Phase Zero’ Human Brain Organoid Platform for Neuroengineering Optical Theranostics | NYC Neuromodulation Online 2020 Available online: https://neuromodec.com/nyc-neuromodulation-online-2020 (accessed on 19 April 2021).

183. Cai, C.; Zambach, S.A.; Grubb, S.; Thomsen, K.J.; Lind, B.L.; Hald, B.O.; Lønstrup, M.; Nielsen, R.M.; Lauritzen, M.J. Impaired Dynamics of Brain Precapillary Sphincters and Pericytes at First Order Capillaries Explains Reduced Neurovascular Functions in Aging 2021, 2021.08.05.455300.